3. SITE 399, 400 AND HOLE 400A

The Shipboard Scientific Party[1]

SITE DATA, SITE 399

Position: 47°23.4′N, 09°13.3′W

Water Depth (sea level): 4399 corrected meters, echo-sounding

Bottom Felt at: 4414 meters, drill pipe

Penetration: 72.5 meters

Number of Cores: 2

Total Core Recovery: 11.77 meters

Percentage Core Recovery: 67.3 per cent

Oldest Sediment Cored:
Depth sub-bottom: 72.5 meters
Nature: Marly calcareous ooze
Age: Pleistocene
Basement: Not reached

Principal Results: Site 399 was drilled as a pilot hole to determine the depth to which casing could be washed during the intended subsequent re-entry hole. Thruster malfunction and beacon signal deterioration forced a move to Site 400, 0.2 km east-southeast (Figure 1) before further drilling could begin. The section penetrated at Site 399 consisted mainly of olive-gray marly calcareous ooze of Pleistocene age.

SITE DATA, SITE 400 AND HOLE 400A

Position: 47°22.9′N, 09°11.9′W

Water Depth (sea level): 4399 corrected meters, echo-sounding

Bottom Felt at: 4399 meters drill pipe

Penetration: 777.5 meters

Number of Holes: 2

Number of Cores: 400(1) 400A(74)

Total Core Recovery: 350.86 meters

Percentage Core Recovery: 48 per cent

Oldest Sediment Cored:
Depth sub-bottom: 768-768.5 meters
Nature: Carbonaceous mudstone and limestone
Age: Late Aptian (Gargasian)
Basement: Not reached

Principal Results: Hole 400A was drilled at the foot of the Meriadzek escarpment of north Biscay in 4399 meters depth of water (Figure 1). The site was located in a half-graben forming part of a succession of tilted and rotated fault blocks near the continent-ocean boundary. The main objectives were to define the nature of the pre-, syn-, and post-rifting environments, the regional unconformities, the paleoceanography and the subsidence history.

Hiatuses were found between the lowermost Pliocene and the uppermost Miocene, within the lower Miocene, between the Oligocene and the middle Eocene, between the upper Paleocene and the Upper Cretaceous, and between the Campanian and the Albian. Four lithologic units and eight sub-units were recognized.

Unit 1 (0-413 m) comprises nannofossil ooze, nannofossil chalks, and marly ooze and chalk which range in age from Holocene to early Miocene. Unit 2 (413-640 m) ranges in ages from early Miocene to late Paleocene. As a whole, this unit is less calcareous and contains a much larger component of siliceous biogenous remains, especially in the middle Eocene. Unit 3 (640-654 m) comprises calcareous and marly nannofossil chalks of late Campanian to Maestrictian age, and is defined at its base by a 30-m.y. hiatus. Unit 4 (654-777.5 m) of Albian to late Aptian age, comprises carbonaceous claystone interbedded with calcareous mudstones. The calcareous mudstones were deposited by turbidity currents whereas the carbonaceous claystone correspond to normal pelagic sediments deposited in a deep environment close to the CCD. The organic matter is carbonaceous material of terrestrial origin. Because no marine organic matter was found, there is no indication that anoxic conditions existed in the Bay of Biscay during the Early Cretaceous. The 30-m.y. hiatus separating the Albian-Aptian "black shales" from the Campanian-Maestrichtian nannofossil chalks is contemporaneous with the well-known global transgression and separates formations which were deposited in deep water.

Within the Tertiary, variations in carbonate, biogenic silica, and clay content along with the observed hiatuses apparently reflect fluctuations in CCD level, bottom current activity, and surface productivity.

BACKGROUND AND OBJECTIVES

The Bay of Biscay is a triangular ocean basin, the shape of which contrasts with the parallel sides of many ocean basins (Figure 2). The Armorican margin of the bay consists of a wide shelf, a slope deeply cut by many canyons, and a broad continental rise that merges with the Biscay abyssal plain; the slope and rise are broken by the Meriadzek Terrace and Trevelyan escarpment. In contrast, the linear slope of the Iberian margin is narrow and cut by few canyons (Berthois and Brenot, 1964; Berthois et al., 1965; Laughton et al., 1975). Two previous DSDP sites, 118 and 119, were

[1]Lucien Montadert (Co-Chief Scientist), Institut Français du Pétrole, Rueil-Malmaison, France; David G. Roberts (Co-Chief Scientist), Institute of Oceanographic Sciences, Surrey, England; Gerard A. Auffret, Centre Océanologique de Bretagne, Brest, France; Wayne D. Bock, Rosenstiel School of Marine and Atmospheric Science, Miami, Florida; Pierre A. Dupeuble, Université de Rouen, Mont-Saint-Aignan, France; Ernest A. Hailwood, University of Southampton, Southampton, United Kingdom; William E. Harrison, University of Oklahoma, Norman, Oklahoma; Hideo Kagami, University of Tokyo, Tokyo, Japan; David N. Lumsden, Memphis State University, Memphis, Tennessee; Carla M. Müller, Geologisch-Paläontologisches Institut der Universität, Frankfurt am Main, Federal Republic of Germany (now at: Institut Français du Pétrole, Rueil-Malmaison, France); Detmar Schnitker, University of Maine, Walpole, Maine; Robert W. Thompson, Humboldt State University, Arcata, California; Thomas L. Thompson, University of Oklahoma, Norman, Oklahoma; and Peter P. Timofeev, USSA Academy of Sciences, Moscow, USSR.

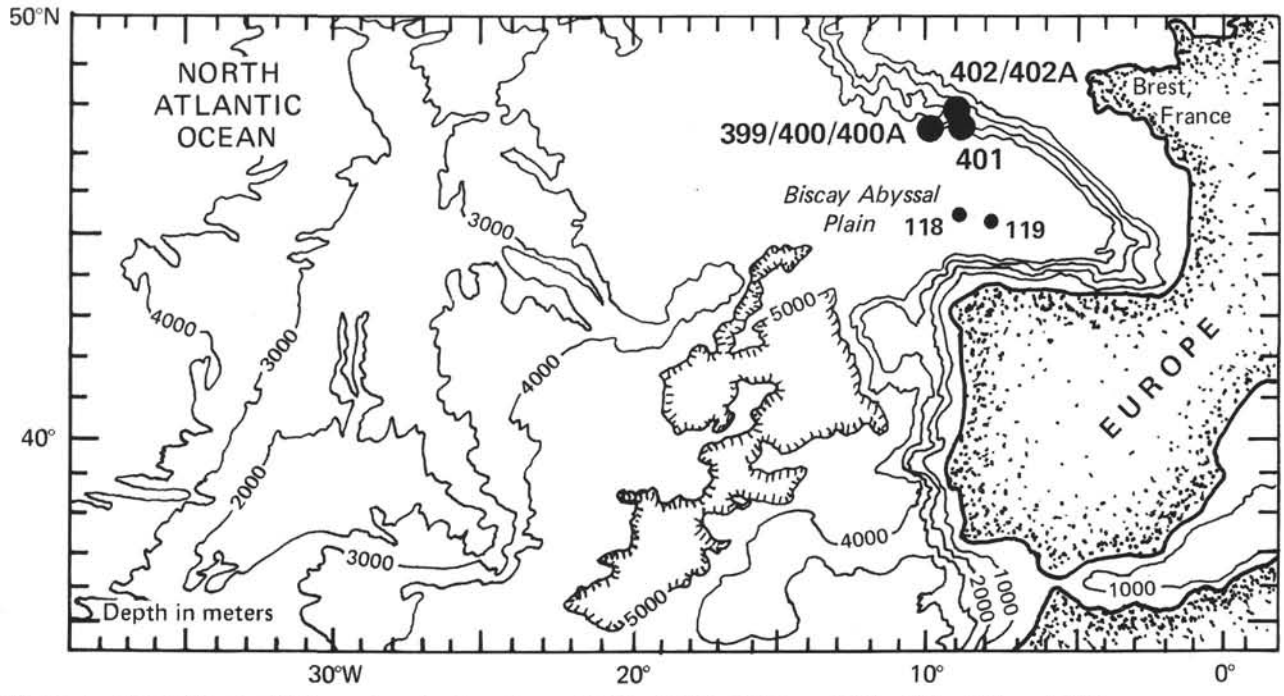

Figure 1. *General map of Biscay showing locations of Holes 400A, 402A, and Sites 401, 118, and 119.*

drilled on the Cantabria seamount that rises above the Biscay abyssal plain (Laughton, Berggren, et al., 1972).

The evolution of the Bay of Biscay and its margins has been the subject of continuing research and discussion since Carey (1955) and Bullard et al. (1965) postulated that it might have formed by the anticlockwise rotation of Spain from Europe. Subsequent paleomagnetic studies have confirmed the rotation of Spain which may have taken place in two phases (Girdler, 1965; Watkins and Richardson, 1968; Van der Voo, 1968; Van der Voo and Zijderveld, 1971; Storetvedt, 1970; Stauffer and Tarling, 1971). Deep crustal studies of the Bay of Biscay, using gravity and seismic refraction techniques, have confirmed the presence of oceanic crust beneath the bay (Bacon et al., 1969; Bacon and Gray, 1971; Limond et al., 1972). Additional evidence for the oceanic nature of the bay is given by the prominent magnetic lineations mapped by Matthews and Williams (1968) and Le Mouel and Le Borgne (1971). However, important differences between the Iberian and Armorican margins have been revealed both by these and other geological and geophysical studies.

From a structural point of view, the Armorican margin and its prolongation in the Aquitaine Basin bears many similarities to other passive margins and consists of a series of horsts and grabens often buried deeply beneath a prograding sedimentary cover. In contrast, the Iberian margin is associated with overthrust structures and gravity tectonics bearing a close spatial relationship to the Pyrenean orogen. The Iberian margin was apparently active between Late Cretaceous and Oligocene-Miocene time (Stride et al., 1969; Cholet et al., 1968; Damotte et al., 1969; Montadert et al., 1971a, b, c, d; Boillot et al., 1971; Montadert and Winnock, 1971; Winnock, 1971; Sibuet and Le Pichon, 1971; Sibuet et al., 1971).

These contrasts in structural style have raised many questions concerning the evolution of the Bay of Biscay and its margins. Questions include the relative importance of the various rifting episodes recorded on land, and the relation between the duration and geometry of the spreading, the Pyrenean deformation, and the subsidence history of the margins. Various hypotheses have addressed these questions. Le Pichon et al. (1971) proposed a rotation of Iberia about a pole near Paris with strike-slip motion of several hundred kilometers along the north Pyrenean fault followed by a Cenozoic compression. Modifications to this hypothesis have been proposed by Choukroune et al., (1973) and by Boillot and Capdevila (1977). In contrast, Montadert and Winnock (1971) have proposed that there was no important strike-slip movement of Iberia and that the Lower Cretaceous distension structures of Biscay and Aquitaine were disturbed by the later Pyrenean movements.

A brief summary of the main events in the evolution of the bay based on geological data from the English Channel, Aquitaine Basin, and the results from DSDP Sites 118 and 119 on the Cantabria seamount (Montadert et al., 1974; Montadert and Winnock, 1971; Curry et al., 1971) follows.

1) Rifting of the Hercynian platform of Europe and North America during Triassic time with thick evaporite deposition in the Aquitaine, Lusitanian, Brand Banks, Celtic Sea, and English Channel basins. Volcanism may also have been important.

2) A period of gentle subsidence of the shallow basin until the upper Malm (Winnock, 1971; Montadert et al., 1974).

3) During the late Malm, regional epeirogenesis (Cimmerian s.l.) associated with minor volcanism began, reaching its maximum intensity during the Early Cretaceous (Albian in the Parentis Basin; Dardel and Rosset, 1971). Evi-

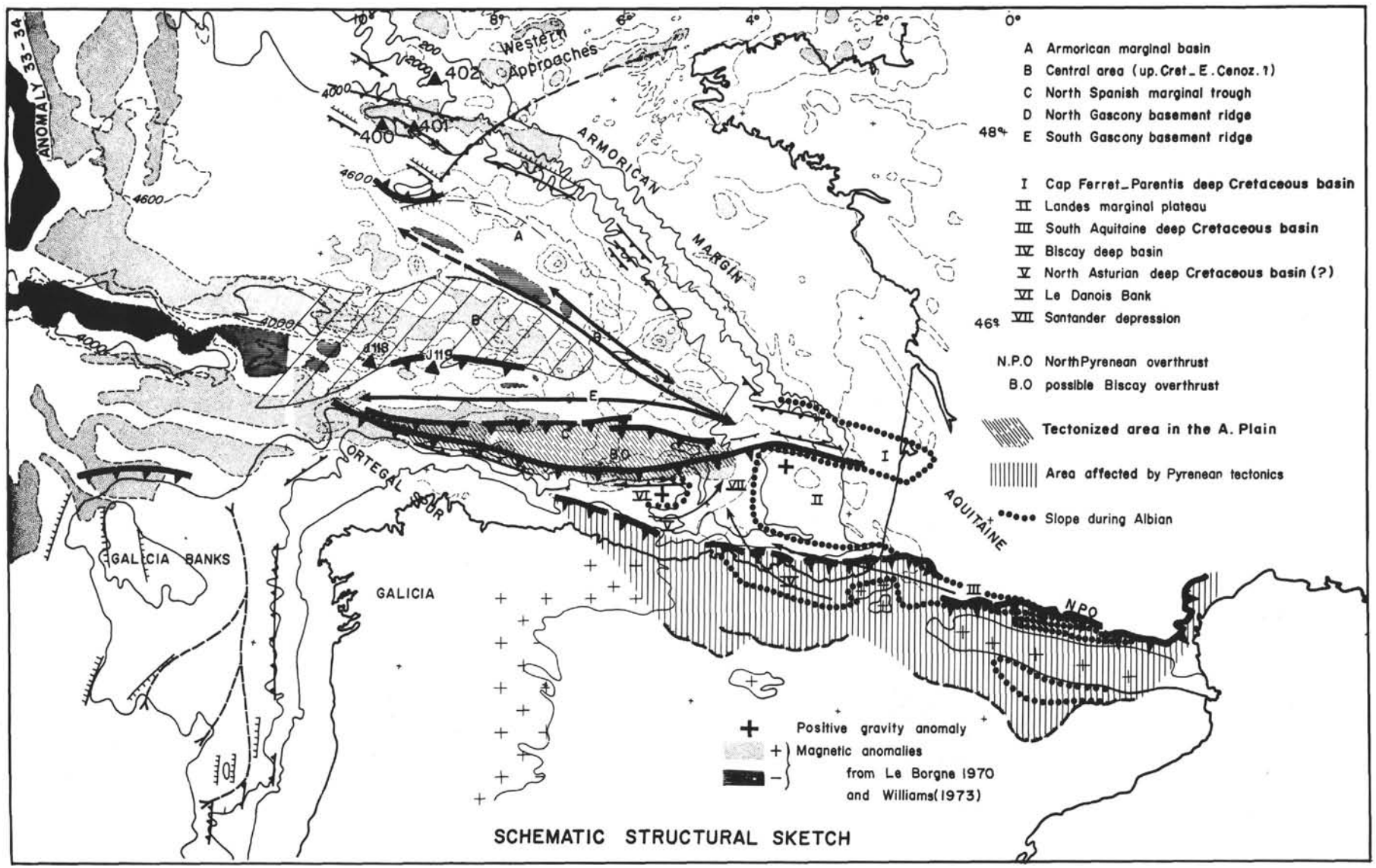

Figure 2. *Tectonic sketch map of the Bay of Biscay.*

dence of the former continuity of the North Atlantic continents up to that time may be given by the absence of *M*-sequence anomalies in the Bay of Biscay and the occurrence of heavy minerals of hypothetical Iberian provenance in the Wealden of southern England.

4) The duration of the opening of the bay and its relationship to the onset of the Pyrenean deformation is not known, but it is clear that strong subsidence of the adjacent platform took place after Early Cretaceous time.

5) Compressive tectonics were initiated at the northern boundary of the Iberian block (North Spanish Trough) in Late Cretaceous time and continued until Oligocene/Miocene time. This compressive phase resulted in the Pyrenean deformation and widespread faulting of early to middle Tertiary age in the abyssal parts of the bay.

6) During the late Tertiary, pelagic sediments were deposited on seamounts (e.g., Cantabria and Bascony seamounts) uplifted during the Pyrenean deformation and thick turbidites were deposited on the marginal depressions and abyssal Bay of Biscay (Montadert et al., 1974; Laughton, Berggren, et al., 1972).

The rifted Armorican margin of the Bay of Biscay has been the subject of several geological and geophysical surveys that have defined the topography, magnetic field, gravity field, and shallow sediment distribution (Stride et al., 1969; Montadert et al., 1971a, b, 1974; Grau et al., 1973; Smith and Van Reissen, 1973; Hersey and Whittard, 1966; Hill and Vine, 1965; Lapierre, 1972; Curry et al., 1971).

Several cruises by the IFP, CNEXO, and CEPM during 1975 and early 1976 dredged sediments, recorded the heat flow, and produced several seismic refraction profiles using sea-bottom seismographs. In addition, about 7000 km of 48-channel and 6-channel seismic profiles were run by IFP-CNEXO-CEPM and the IOS, respectively. The purpose of these surveys was to provide a comprehensive regional picture of the margin to extend interpretation of the drilling and to define site locations precisely.

To the south of Brittany, the sedimentary cover on the Armorican shelf forms a homocline that becomes progressively thicker offshore and is affected by a few northeast-southwest-trending faults and undulations representing the offshore prolongation of structures known on land between northern Aquitaine and Brittany. In this area, the Hercynian basement is overlain by Paleogene deposits, in turn overlapped by Neogene sediments in the west.

In the southwest the shelf is underlain by the wide Western Approaches or western English Channel Basin. The large Alderney-Ushant fault, which affects the pre-Mesozoic basement and its cover, divides the basin into two geological provinces. To the south of the fault, the pre-Mesozoic basement is covered by thin or patchy sediments of Cretaceous and Cenozoic age. To the north, the section is much thicker and includes beds of Permo-Triassic to Cenozoic age. In the basin, southwest-trending folds that bring the Mesozoic to the sea bed are associated with strong southwest-trending magnetic anomalies. Between Permo-Triassic and Jurassic time, continental and then marine sediments were deposited in a half-graben limited to the south by the Alderney-Ushant fault. During the Late Jurassic and Early Cretaceous, these beds were folded and faulted by distensive movements which may be linked with the opening of the Bay of Biscay. During the Early Cretaceous, thick deltaic sands (Wealden facies) were contemporaneously deposited in both the English Channel and Celtic Sea basins. The "Cenomanian" transgression has preserved the irregular erosion surface formed by these movements as a marked unconformity. Renewed movements in the basin took place between Danian and Ypresian time and again between Oligocene and Miocene time. The latter event was associated with downwarping and renewed faulting. A schematic section across the English Channel and Celtic Sea basins is given in Figure 3.

The multichannel seismic surveys of the deeply dissected slope show that it is underlain by thin prograding sediments that rest on a series of rifted blocks and half-grabens that trend sub-parallel to the margin (Montadert et al., 1971b, Montadert et al., this volume). Montadert et al. (1971, 1974), have subdivided the sedimentary cover into seismic Units 1, 2, and 3. Units 1 and 2 were penetrated at DSDP Sites 118 and 119 on the Biscay abyssal plain (Laughton, Berggren, et al., 1972).

Unit 1 is post-Eocene to Quaternary in age and its base correlates with the end of the normal faulting episode observed locally beneath the margin and, more widely, beneath the abyssal plain. At Sites 118 and 119, the principal lithologies consist of turbidites interbedded with pelagic sediments. At the shelf break, the unit is 600 to 800 meters thick, and has the structure of a prograding sedimentary talus. Beneath the slope, the unit is of variable thickness and contains both slump structures and sediment drifts.

Unit 2 is of early Tertiary to Late Cretaceous age. At Sites 118 and 119, it is composed of marls and calcarenites in its upper part. At the shelf break, it is 800 to 1000 meters thick, but thickens beneath the slope. The lithology of the lower part of the unit is not known.

Unit 3 is overlain unconformably by Unit 2 and its base may be defined in part by an erosional unconformity. Beneath the slope the unit appears to infill the half-grabens or is thinly draped over the fault blocks, but beneath the abyssal plain and Amorican marginal basin the unit rests unconformably on oceanic crust.

The basement underlying the slope consists of a series of tilted and rotated fault blocks containing well-developed reflectors. Close to the continent-ocean boundary beneath the Trevelyan escarpment, the basement is opaque.

Dredging in the region (Pastouret et al., 1974; Pastouret and Auffret, 1975; Pautot et al., 1976; Boillot et al., 1971) has yielded mostly middle Eocene to Miocene chalky limestone, although Montadert et al. (1974) reported a core of Albian algal limestone. A summary of more recent dredgings is given by Auffret et al. (this volume). The oldest dredged rocks are granites of Hercynian aspect (Pautot et al., 1976). In addition, Tithonian calpionellid limestones, Lower Cretaceous neritic and reefal sediments, and conglomerates containing fragments of Permo-Triassic sandstone have been dredged. One suite of dredged rocks exhibits a transition from Barremian beige and green marls, of external platform facies, to Albian-Aptian black marls

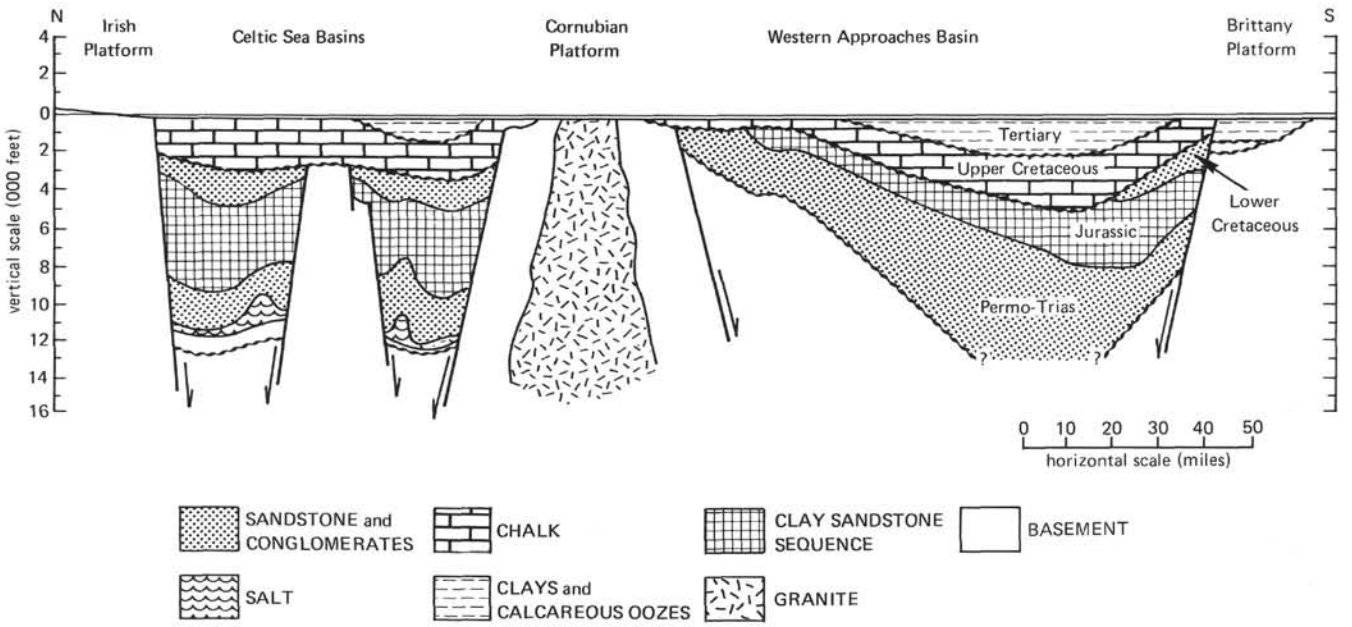

Figure 3. *Schematic section across the English Channel and Celtic Sea basins (after Naylor and Mounteney, 1977).*

and bioclastic limestones characteristic of the infratidal zone. These sediments were recovered near fault blocks, and their position with respect to Unit 3 is unclear for they may represent either Unit 3, or sediments from within the fault block, or reefal sediments confined to the crests of the blocks. The variable lithologies and the fault block-controlled distribution of Unit 3 suggest that important facies changes may be present.

The multichannel seismic surveys and the limited geological data derived from dredge hauls show that the margin was rifted and that subsequently it has subsided to its present depth. In contrast to the thickly sedimented margins off eastern North America, for example, pre-rift sediments were preserved in fault blocks at shallow depths below the sea floor under a thin cover of post-rift sediments. Drilling within the capabilities of *Glomar Challenger* thus offered the opportunity to obtain a complete record of the structural and stratigraphic evolution of a starved, passive, rifted margin. Within this broad objective, it was also intended to examine the following problems of particular relevance to passive margins.

Nature of the Pre- and Post-Rifting Environments

It is clear from the geological history of western Europe and offshore Canada, that the North Atlantic continents were subjected to regional distension during Triassic time that shaped the epicontinental basins of the Jurassic period; within these basins, the main rifting took place. A principal objective of drilling into the pre-rift sediments was to establish the age and facies of pre-rift, syn-rift, and immediately post-rift sediments to clarify the environment and duration of rifting. In this respect, it was important to establish whether the rifting involved submarine or subaerial uplift with or without volcanism and thus the validity of the widely used East African Rift System-Gulf of Aden analogy.

Regional Unconformity

Beneath many passive margins, a regional unconformity marks a transgressive phase associated with the termination of faulting. It has been postulated that this unconformity marks the end of "pull apart" associated with rifting and the onset of subsidence associated with the accretionary spreading process. Penetration of the unconformity at the base of Unit 3 would help define the altitude of the continent at the onset of subsidence. In a more regional context, confirmation of this hypothesis as a means of indirectly dating the onset of spreading is of obvious relevance to margin geology and the evolution of the North Atlantic Ocean.

Subsidence

Although the dredged neritic and reefal sediments clearly show that the margin has subsided, the rate is unknown, as are the possible effects of the mid-Tertiary movements recorded in the Western Approaches Basin and Biscay abyssal plain. The subsidence history of the site may also contribute to a better understanding of the complex relationships between uplift, subsidence, regression, and transgression in relation to spreading rate changes.

Comparative Facies Studies

The comparative lithologies of upper-slope, mid-slope, and rise sediments of the Tertiary and Cretaceous provided by the drilling transect should aid definition of the facies relationships on continental margins.

Paleoceanography

The sediments of continental margins are anticipated to record changes in vertical and horizontal oceanographic gradients as a function of both time and space. Identification of depth specific and water specific sedimentary facies help

determine the changing environmental conditions in the widening North Atlantic Ocean. Environmental changes of special interest to margin studies include the Cenozoic changes in bottom water circulation, variations in the elevation of the CCD, and the influence of oxygen minima in black shale deposition in Cretaceous time.

Diagenesis

In addition to an examination of the diagenesis of clay, carbonate, and siliceous sediments, the maturation of organic matter in relation to changing thermal conditions through rifting and subsidence is a prime objective.

Paleomagnetism

The principal objective is to correlate the magnetic reversal history with biostratigraphic zonations based on foraminifers, nannofossils, and palynological data.

Site 400 (Figures 1, 3, 4, 5a, and 5b) is located at SP300 on profile OC412, close to SP345 on the intersecting profile OC414. The site is situated in a basinal position between two fault blocks tilted along rotational faults trending east-northeast — west-southwest. The northernmost fault controls the southern edge of the Meriadzek Terrace. To satisfy safety considerations, the site was positioned away from the crest of the tilted block in an area where the flat-lying attitude of the reflectors was confirmed by the intersecting profile. At the site, the important regional unconformity separating syn- and post-rift sediments lies at the shallow depth of 660 to 744 meters, inferred from sonobuoy and velocity data. Although these depths lay within the single bit capability of *Glomar Challenger*, it was decided that weather risks and possible bit failure in unknown lithologies merited drilling the hole using the re-entry to ensure successful completion of the hole and the important logging program.

SITE APPROACH AND DRILLING OPERATIONS

The approach to Site 399 (Figure 6) involved proceeding along a heading of 257 degrees, well north of the site, before a southward turn along 191 degrees to follow along the control seismic line 1FPOC412 which crosses the site. A satellite fix at 0010 hours LCT/May 24 confirmed the position about five miles west-northwest of the designated site. The vessel continued southward and at 0125 hours LCT turned east to a heading of 011° reckoned to cross the site at which a 16-KHz beacon was dropped at 0200 hours LCT. The beacon failed shortly after the ship was positioned and another 13.5-KHz beacon was dropped at the site. Between 0400 and 0845 hours LCT, positioning on the beacon was hampered by a weak signal and successive computer failures. To enhance the beacon signal, two offsets of 800 feet north and 600 feet west and 1200 feet north and 900 feet west were made at 2130 and 2200 hours LCT. These resulted in some improvement in signal strength. A final offset for the drill site was 800 feet north and 600 feet west, the site being about a quarter of a mile west-northwest of the initial target at shot point 300 on line OC412. Fixes obtained while on site gave a position of 47°23.40'N, 09°13.3'W (average of five good fixes).

The initial hole was spudded at 2345 hours on 25 May in 4399 meters of water. Pilot testing began and the hole was washed to a depth of 4477 meters below the derrick floor; Core 2 was cut from 4477 to 4486.5 meters. By 2000 hours on 24 May, it had become difficult to maintain position because of beacon signal deterioration. In view of this, the ship was moved 3000 feet east-southeast along strike to Site 400 out of range of the first beacons and a new 16-KHz double life beacon was deployed. Satellite fixes showed the vessel to be about 0.1 mile east-southeast of the initial target.

At 1015 hours on 25 May, the pilot hole at Site 400 was spudded in a water depth of 4399 meters. Pilot testing began and the hole was washed to a depth of 4478 meters below the derrick floor.

After tripping the drill string at Site 400, the re-entry cone for Hole 400A was rigged and keel-hauled at 0045 hours on 26 May. Casing was hung in the cone and the whole assembly bottomed at 1745 hours on 26 May. The first core (4473.5-4483.0 m) was cut at 0430 hours on 27 May and thereafter cores were taken continuously (Table 1). Core recovery was poor despite repeated mud spotting; younger lithologies occurring as fragments in the core strongly suggested downhole contamination and failure to flush out the hole. After Core 60, recovery improved, which may have been related to the harder Upper Cretaceous chalks then being drilled. An inclinometer test on Core 60 gave a value of 7°45'. Through 1 and 2 June, recovery was often less than 5 per cent, and abnormally high pump pressures of 1300 pounds were being used to drill ahead. Attempts to unplug the bit failed and it was decided to trip the drill string, check the bit, and re-enter. On completing the trip, the casing hanger was removed and a new bit and bit release mechanism incorporated in the bottom hole assembly to enable logging on completion of the hole. Re-entry began at 0730 hours on 3 June and accomplished successfully at 1050 hours on 3 June. Three stands of pipe were then run to verify re-entry prior to running pipe. At this time (1650 hours) the pin in the pup joint attached to the Bowen sub failed and the entire drill string was lost. After laying down the remaining drill pipe extracted from the hole, *Glomar Challenger* departed for Site 401 in the afternoon of 5 June.

LITHOLOGY

The upper 640 meters of section penetrated at Sites 399 and 400 consist principally of nannofossil ooze, nannofossil chalk, and marly nannofossil chalk ranging in age from late Paleocene to Recent (Figure 7). A prominent hiatus between the lower Oligocene and middle Eocene was encountered at a sub-bottom depth of 515 meters, and upper Paleocene orange-pink marly chalk was found resting on Maestrichtian white chalk at a depth of about 640 meters. Only about 15 meters of Upper Cretaceous sediment occur in Hole 400A and they rest on interbedded carbonaceous mudstone, calcareous mudstone, and marly nannofossil chalk of Albian age. Upper Aptian carbonaceous mudstones were reached at a sub-bottom depth of 712.0 meters and the hole was terminated by the drill string separation at 777.5 meters.

The sedimentary succession encountered at these sites is subdivided into four lithologic units and eight sub-units (Table 2, Figure 7) described below in descending order.

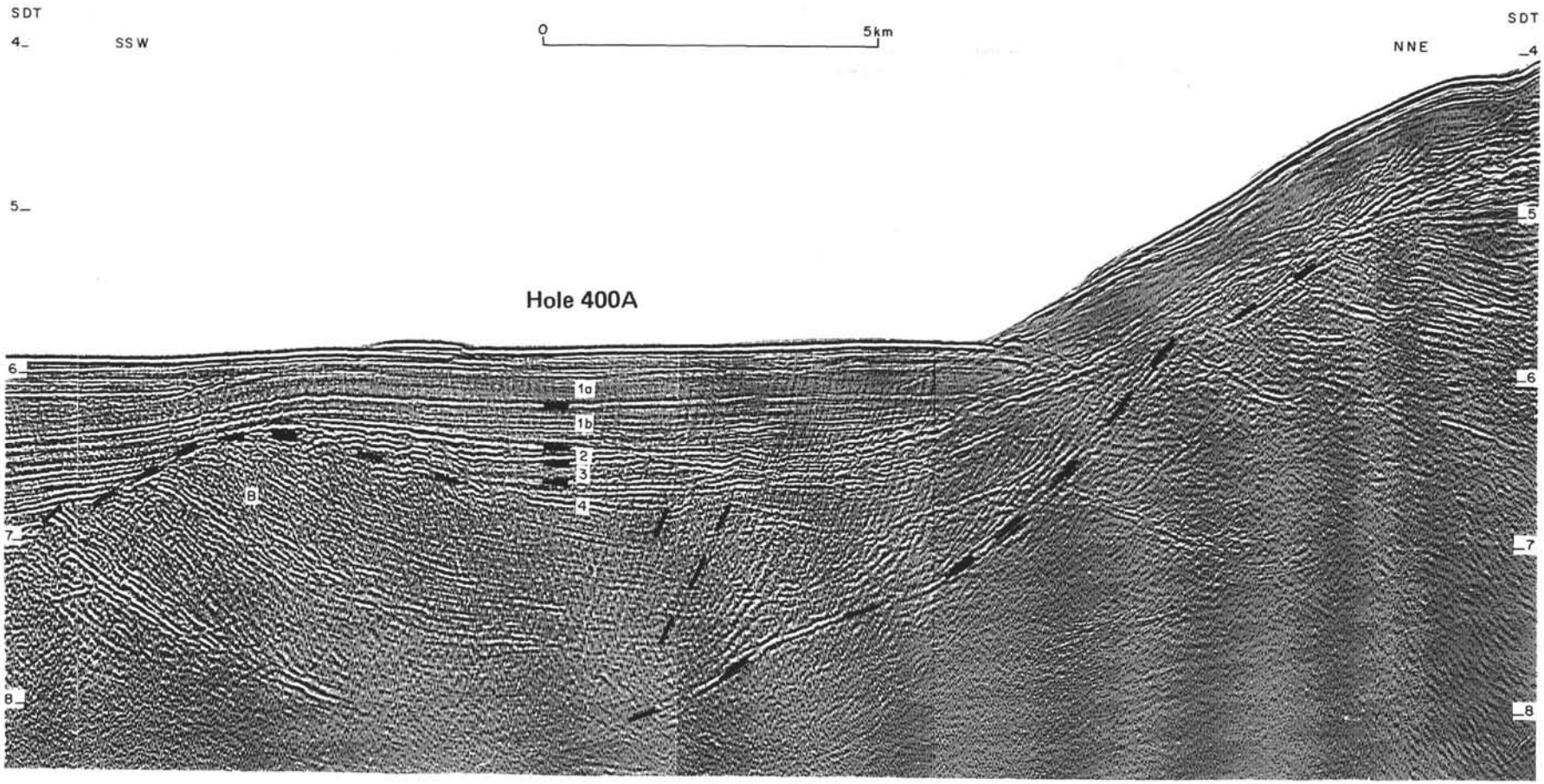

Figure 4. *Multichannel seismic profile IFP-CNEXO-CEPM OC 412 through Hole 400A (CDP 24, migrated). 1a-1b = Post Eocene Cenozoic, 2 = Upper Cretaceous to Eocene, 3 = Aptian/Albian, 4 = Syn-rifting sediments, B = Pre-rift sediments.*

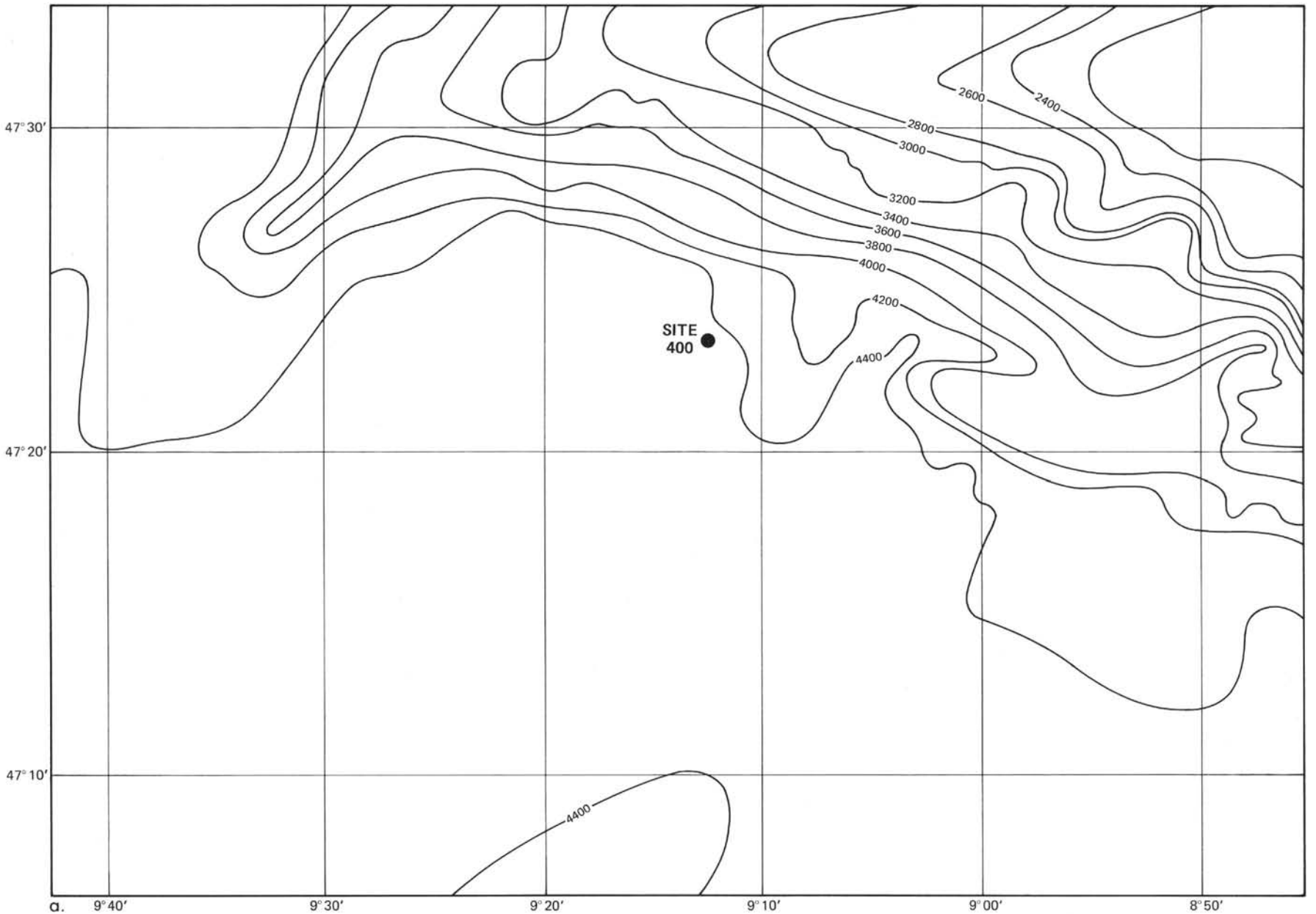

Figure 5a. *Bathymetry in the vicinity of Site 400 from Berthois.*

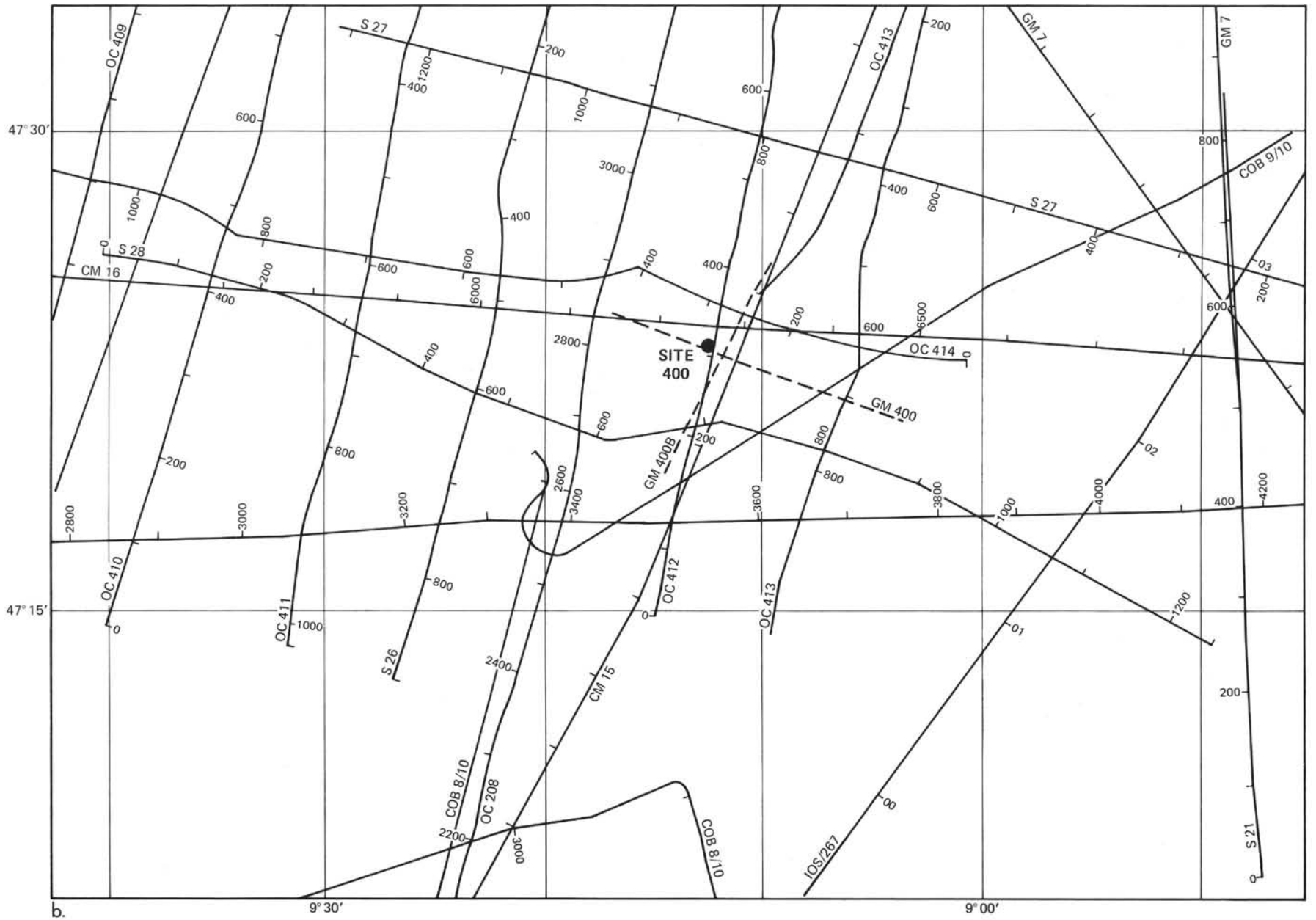

Figure 5b. *Location of seismic profiles around Site 400. OC, GM, S = Multichannel seismic profile IFP-CNEXO-CEPM, GM 400-400B = High-resolution multichannel seismic profile IFP-CNEXO-CEPM, CM = Multichannel seismic profile IOS, COB, IOS = Single-channel seismic profile.*

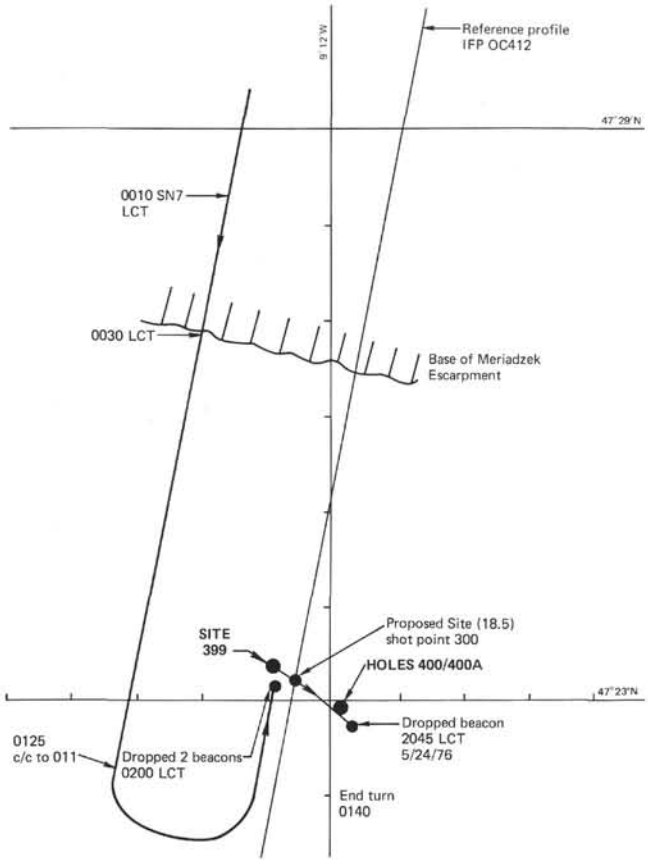

Figure 6. *Approach of* Glomar Challenger *to Hole 400A.*

Cenozoic Units

Unit 1

Lithologic Unit 1 extends from the sea floor to sub-bottom depth of 413 meters. The principal sediment types comprising the unit include light bluish gray nannofossil ooze, nannofossil chalks, and greenish gray marly ooze and chalk which range in age from Holocene to early Miocene. Calcium carbonate, chiefly in the form of nannofossils, constitutes in excess of 50 per cent of the sediment through most of the section and ranges above 90 per cent in the middle Miocene. Detrital clay-sized material, chiefly illite and smectite, comprises most of the remainder. The principal compositional variations in the unit relate to changes in the $CaCO_3$/clay ratio and the frequency of marly beds. On this basis, two sub-units have been distinguished. In addition, however, definite trends in clay mineralogy are evident in the unit.

Sub-unit 1A consists of a sequence of alternating nannofossil ooze and marly ooze of Holocene to late Pliocene age. It is distinguished from Sub-unit 1B largely on the basis of the generally lower $CaCO_3$ content, higher detrital quartz, presence of frequent interbeds of marly calcareous ooze, and occasional occurrence of calcareous mud. Compositionally the sediments have a general range of 20 to 70 per cent (averaging about 50 to 60%) $CaCO_3$, most of which is nannofossils. Detrital clay-sized material accounts for 25 to 50 per cent of the sediment; the other common constituents, foraminifers and siliceous microfossils, make up less than 10 per cent. The clay mineral suite is dominated by illite and mixed-layer clay, but chlorite and kaolinite persist in the clay fraction in concentrations to the order of 10 to 20 per cent.

Fluctuations in the clay/carbonate ratio are reflected in the section by variations in color. The carbonate-rich nannofossil oozes are generally greenish gray or light bluish gray. These occur in beds 0.5 to 1 meter thick separated by olive-gray to brownish gray marly zones 25 to 50 cm thick or less. In many cases the marly zones in turn are color banded on a still smaller scale (5-10 cm), again reflecting slight variations in carbonate/clay ratio and degrees of oxidation. All lithologies show evidence of moderate to intense bioturbation.

At Site 400, the uppermost 1.1 meters of sediment consist of alternating greenish gray nannofossil ooze and grayish orange diatomaceous nannofossil ooze of late Quaternary age. Nannofossils, with a smaller but significant admixture of foraminifers and diatoms, make up 70 to 80 per cent of these sediments, whereas this biogenous component drops to 50 per cent or less in the immediately underlying olive-gray marly calcareous oozes and muds. A detrital fraction consisting chiefly of clay minerals, quartz, and calcite with minor amounts of glauconite and dolomite constitutes between 60 and 90 per cent of these sediments. At Site 399, the sequence is similar although the uppermost biogenous unit is only 45 cm thick and lacks the diatomaceous layers.

Sub-unit 1B is comprised mostly of a light bluish gray to bluish white nannofossil ooze and chalk. These sediments range in age from late Pliocene to early Miocene and were encountered between sub-bottom depths of 130 to 413 meters. The transition from ooze to chalk occurs in the lower Pliocene at a sub-bottom depth of about 190 meters. Intercalated through most of the section are greenish gray marly nannofossil oozes and chalks. Typically, these range between 20 and 30 cm thick and occur at intervals of from 1 to 3 meters.

Nannofossils are the major constituent in this section, generally making up 60 to 70 per cent of the sediment but ranging as high as 80 to 85 per cent in the upper Miocene portion (240-260 m) and near the middle to upper Miocene boundary (320-380 m). The principal auxiliary components are detrital clay and quartz which together average 20 to 30 per cent. Foraminifers are common (up to 10%) in that part of the unit above about 240 meters, but were not observed in more than trace quantities below. Siliceous microfossils, in particular sponge spicules, occur sporadically with notable concentrations (5% or more) in the intervals 195 to 220 meters, and 260 to about 320 meters.

The entire section bears evidence of moderate to intense bioturbation. Trace fossils identified through much of the section include *Zoophycos, Teichichnus,* and halo, composite, and rind burrows. These are generally distinguished by darker colors, pyrite concentrations, and the presense of abundant fecal pellets. Such bioturbation appears to be particularly pronounced in association with greenish gray marly layers.

Analyses of $CaCO_3$, X-ray mineralogy, and smear-slide examinations divulge several compositional trends which may be significant in terms of paleoceanographic conditions. First is the previously mentioned general trend of increasing $CaCO_3$ content downward through the unit

TABLE 1
Coring Summary, Sites 399 and 400

Core	Date (May 1976)	Time	Depth From Drill Floor (m)		Depth Below Sea Floor (m)		Length Cored (m)	Length Recovered (m)	Recovered (%)
Site 399									
1	24	0125	4414.0	4422.0	0	8.0	8.0	8.0	100
2	24	0930	4477.0	4486.5	63.0	72.5	9.5	3.77	42
Hole 400									
1	25	1140	4399.0	4408.0	0	9.0	9.0	9.0	100
Hole 400A									
1	27	0545	4473.5	4483.0	74.5	84.0	9.5	1.95	20
2	27	0715	4483.0	4492.5	84.0	93.5	9.5	8.7	90
3	27	0840	4492.5	4502.0	93.5	103.0	9.5	5.69	58
4	27	1010	4502.0	4511.5	103.0	112.5	9.5	7.45	77
5	27	1145	4511.5	4521.0	112.5	122.0	9.5	1.96	21
6	27	1330	4521.0	4530.5	122.0	131.5	9.5	4.45	45
7	27	1502	4530.5	4540.0	131.5	141.0	9.5	4.19	48
8	27	1650	4540.0	4549.5	141.0	150.5	9.5	8.96	95
9	27	1820	4549.5	4559.0	150.5	160.0	9.5	9.5	100
10	27	2000	4559.0	4568.5	160.0	169.5	9.5	3.85	40
11	27	2133	4568.5	4578.0	169.5	179.0	9.5	2.31	23
12	27	2308	4578.0	4587.5	179.0	188.5	9.5	9.37	99
13	28	0030	4587.5	4597.0	188.5	198.0	9.5	7.3	77
14	28	0215	4597.0	4606.5	198.0	207.5	9.5	4.17	44
15	28	0355	4606.5	4616.0	207.5	217.0	9.5	6.57	68
16	28	0520	4616.0	4625.5	217.0	226.5	9.5	0.88	9
17	28	0701	4625.5	4635.0	226.5	236.0	9.5	7.5	78
18	28	0830	4635.0	4644.5	236.0	245.5	9.5	9.58	100
19	28	1005	4644.5	4654.0	245.5	255.0	9.5	6.56	68
20	28	1220	4654.0	4663.5	255.0	264.5	9.5	8.24	87
21	28	1352	4663.5	4673.0	264.5	274.0	9.5	6.01	68
22	28	1530	4673.0	4682.5	274.0	283.5	9.5	5.85	61
23	28	1701	4682.5	4692.0	283.5	293.0	9.5	6.82	75
24	28	1850	4692.0	4701.5	293.0	302.5	9.5	8.94	94
25	28	2027	4701.5	4711.0	302.5	312.0	9.5	9.39	98
26	28	2222	4711.0	4720.5	312.0	321.5	9.5	3.96	44
27	29	0030	4720.5	4730.0	321.5	331.0	9.5	0.6	6
28	29	0222	4730.0	4739.5	331.0	340.5	9.5	0.2	2
29	29	0410	4739.5	4749.0	340.5	350.0	9.5	1.64	17
30	29	0550	4749.0	4758.5	350.0	359.5	9.5	1.61	17
31	29	0730	4758.5	4768.0	359.5	369.0	9.5	1.35	13
32	29	0915	4768.0	4777.5	369.0	378.5	9.5	2.14	22
33	29	1005	4777.5	4787.0	378.5	388.0	9.5	0	0
34	29	1410	4787.0	4796.5	388.0	397.5	9.5	0.11	1
35	29	1542	4796.5	4806.0	397.5	407.0	9.5	4.50	45
36	29	1825	4806.0	4815.5	407.0	416.5	9.5	2.43	25
37	29	2017	4815.5	4825.0	416.5	426.0	9.5	5.84	62
38	29	2237	4825.0	4834.5	426.0	435.5	9.5	1.91	20
39	30	0045	4834.5	4844.0	435.5	445.0	9.5	4.09	43
40	30	0245	4844.0	4853.5	445.0	454.5	9.5	3.03	31
41	30	0428	4853.5	4863.0	454.5	464.0	9.5	0.61	6
42	30	0605	4863.0	4872.5	464.0	473.5	9.5	0.16	1
43	30	0745	4872.5	4882.0	473.5	483.0	9.5	7.45	78
44	30	0945	4882.0	4891.5	483.0	492.5	9.5	1.73	18
45	30	1145	4891.5	4901.0	492.5	502.0	9.5	7.14	75
46	30	1415	4901.0	4910.5	502.0	511.5	9.5	4.15	44
47	30	1632	4910.5	4920.0	511.5	521.0	9.5	9.71	100
48	30	1858	4920.0	4929.5	521.0	530.5	9.5	3.15	33
49	30	2147	4929.5	4939.0	530.5	540.0	9.5	5.68	58
50	30	2352	4939.0	4948.5	540.0	549.0	9.5	5.99	63
51	31	0200	4948.5	4958.0	549.0	559.0	9.5	9.75	100
52	31	0350	4958.0	4967.5	559.0	568.5	9.5	7.32	77
53	31	0530	4967.5	4977.0	568.5	578.0	9.5	1.90	20
54	31	0720	4977.0	4986.5	578.0	587.5	9.5	4.36	45
55	31	0946	4986.5	4996.0	587.5	597.0	9.5	2.69	28
56	31	1214	4996.0	5005.5	597.0	606.5	9.5	2.41	25
57	31	1530	5005.5	5015.0	606.5	616.0	9.5	2.01	21
58	31	1755	5015.0	5023.5	616.0	624.5	8.5	0.1	1
DRLD	31		5023.5	5024.5	624.5	625.5	1.0	-	-
59	31	2023	5024.5	5034.0	625.5	635.0	9.5	1.04	11
60	31	2200	5034.0	5043.0	635.0	644.5	9.5	9.53	100

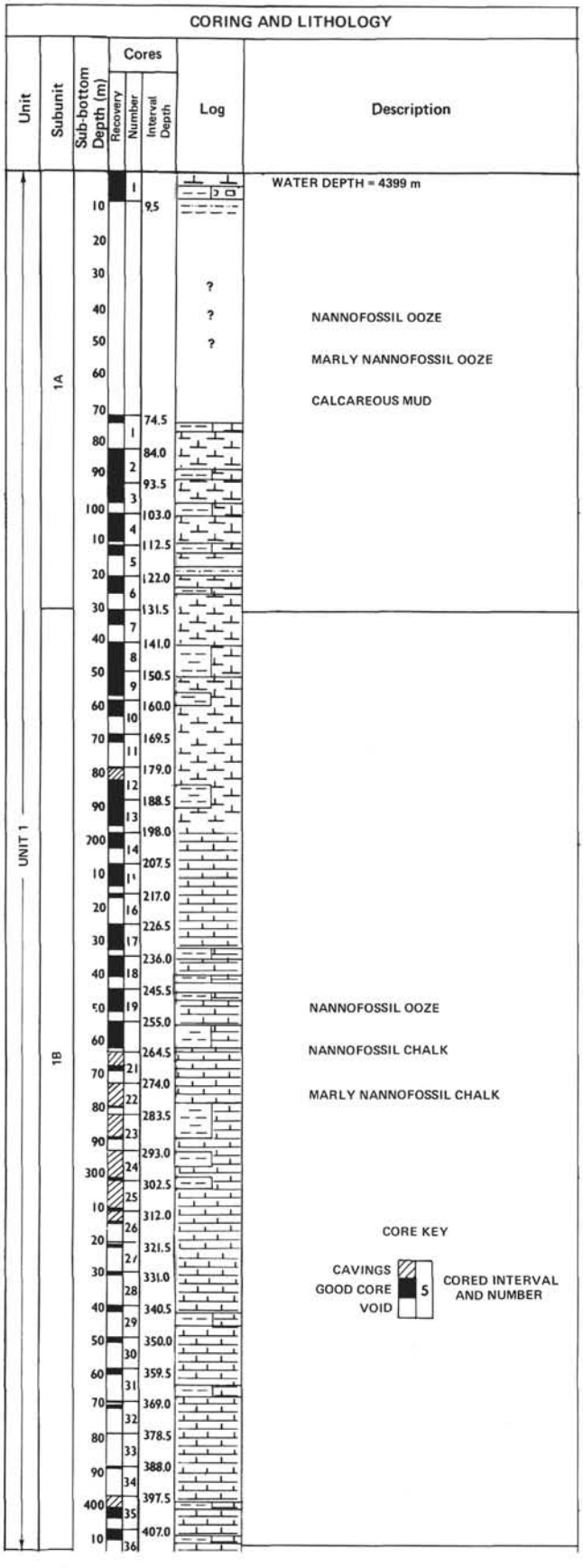

Figure 7. *Lithologic summary of Hole 400A.*

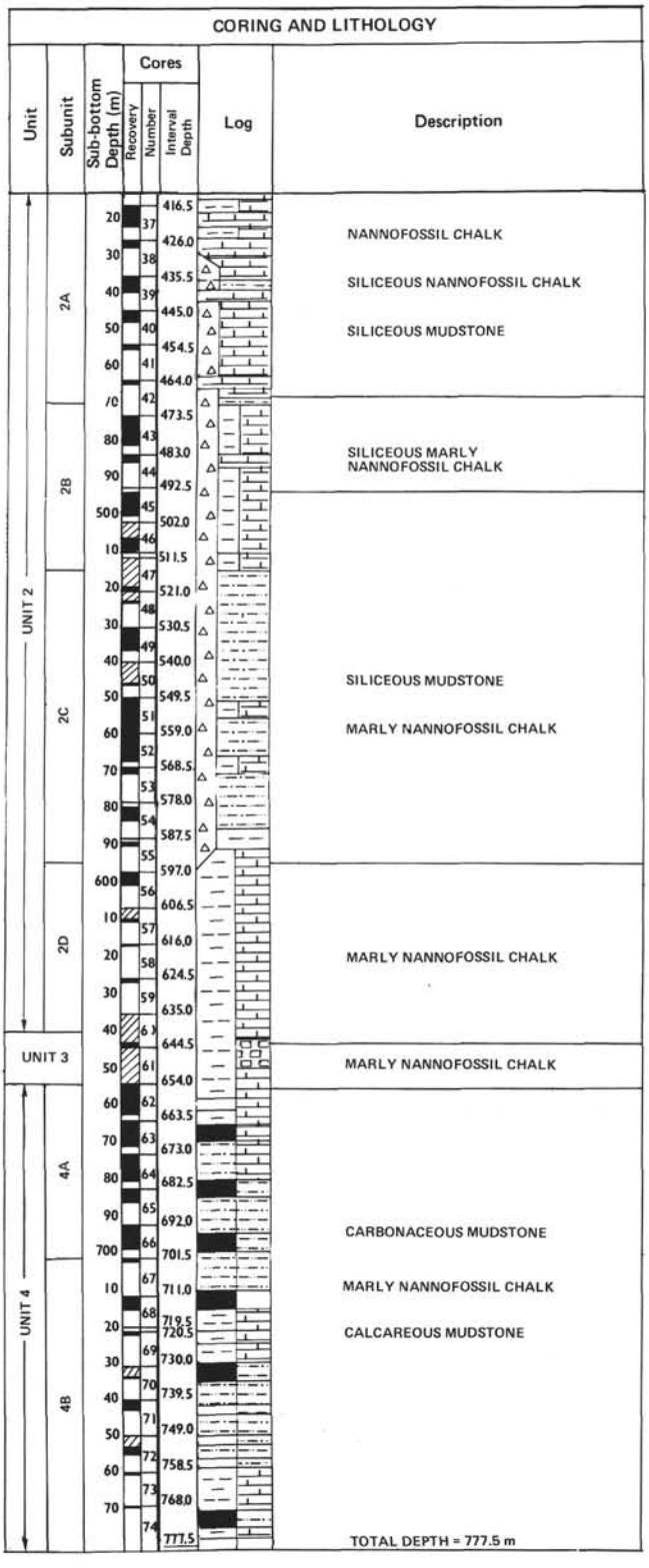

Figure 7. *(Continued).*

with maximum concentrations observed in the middle Miocene portion (Cores 27-32, 320-380 m). Second are perturbations in the $CaCO_3$/clay ratio which are superimposed on this general trend (Figure 7). Thus a possible secondary $CaCO_3$ maximum appears at depths

TABLE 2
Lithologic Units, Sites 399, 400, and Hole 400A

Unit	Cores	Depth Below Sea Floor (m)	Lithology	Age
1A	1-6	0-130	Nannofossil ooze, marly nannofossil ooze, calcareous mud	Quaternary-late Pliocene
1B	7-36	130-413	Nannofossil ooze, nannofossil chalk, marly nannofossil ooze	Late Pliocene-early Miocene
2A	37-42	413-470	Nannofossil chalk, siliceous nannofossil chalk, siliceous mudstone	Early Miocene
2B	43-47	470-515	Siliceous marly, nannofossil chalk	Early-late Oligocene
			HIATUS	
2C	47-55	515-595	Siliceous mudstone, marly nannofossil chalk	Early-middle Eocene
2D	56-59	595-640	Marly nannofossil chalk	Late Paleocene-early Eocene
			HIATUS	
3	60-61	640-654	Nannofossil chalk	Late Cretaceous (Maestrichtian/Campanian)
			HIATUS	
4A	62-67	654-711	Carbonaceous mudstone, marly nannofossil chalk, calcareous mudstone	Early Cretaceous (Albian)
4B	68-74	711-777.5	Carbonaceous mudstone, marly nannofossil chalk, calcareous mudstone	Early Cretaceous (late Aptian)

between 190 and 250 meters and a slight minimum between 250 and 300 meters. Associated with the minimum is a slight peak in biogenous SiO_2 concentration. There are substantial variations in the clay mineral suite. In the upper part of the unit the clay mineral suite is dominated by illite and mixed layer illite-smectite. As in Sub-unit 1A, kaolinite and chlorite constitute a persistent fraction of about 10 to 20 per cent each. Downward in the section, mixed layer clay disappears, chlorite shows a steady decline to about 5 per cent, and smectite undergoes a corresponding increase in abundance. These trends are accompanied by a general decline in quartz content.

Unit 2

Lithologic Unit 2 extends from a sub-bottom depth of 413 to 640 meters (Cores 37-60) and ranges in age from early Miocene to late Paleocene. The base of the unit corresponds with a 7.5-m.y. hiatus between yellowish brown upper Paleocene marly chalk above and white marly chalk of Maestrichtian age below. A prominent lower Oligocene-middle Eocene hiatus occurs within the unit. Considered as a whole, this unit differs from Unit 1 in being less calcareous and containing a much larger component of siliceous biogenous remains, in particular, sponge spicules. Furthermore, Unit 2 is characterized by a striking alteration of sediment color, ranging from yellowish brown and pink in the Paleocene, lower Eocene, and Oligocene to greenish gray and light bluish gray in the middle Eocene and lower Miocene. The brown to pink parts of the section have exceptionally high values of magnetic intensity which notably are accompanied by slight peaks in the detrital quartz content. The boundary between Units 1 and 2 was picked in Core 36 where siliceous remains first show a marked and sustained increase. Smectite shows a substantial increase at the expense of the other clay minerals at about this same depth and both drilling rate and sonic velocity characteristics change significantly. Four sub-units (2A-D) have been differentiated in Unit 2, largely on the basis of variations in biogenous silica, carbonate, and prevalent sediment color. The clay mineral suite remains fairly uniform throughout the unit and is dominated by smectite (50-60%) with a persistent admixture of illite (20-30%), kaolinite (10-15%), and chlorite (<10%).

Sub-unit 2A (upper part) is dominated by interbedded marly chalk and nannofossil chalk of early Miocene age. Prevalent colors in these sediments are light bluish gray, greenish gray, and dusky-yellow-brown, and these alternate in beds on the order of 10 to 20 cm thick. Boundaries between the various lithologic types have been smeared and disrupted by intense bioturbation so that a complex coloration pattern is characteristic. Downward in the section, siliceous remains, chiefly sponge spicules, increase in abundance and the lithology changes to a predominance of bluish gray siliceous nannofossil chalk with occasional interbeds of greenish gray siliceous mudstone. Sponge spicules comprise the order of 10 to 20 per cent of the sediments and, in a number of places, they range as high as 40 per cent where they have been concentrated to form distinct, laminated lenses a few millimeters to one centimeter thick. Nannofossils account for 30 to 50 per cent, most of the remaining sediments consisting of detrital clay (chiefly smectite) and quartz (5-10%).

Sub-unit 2B occurs at sub-bottom depths between 470 and 515 meters and ranges in age from early to late Oligocene. Lithologically the unit is similar to 2A, consisting dominantly of siliceous marly nannofossil chalk. In contrast to the predominance of olive-gray and green colors in the overlying and underlying sediments, however, yellowish gray, yellowish brown, and grayish orange prevail. Siliceous biogenous remains decrease somewhat within the chalks of this unit compared to those above and below, where $CaCO_3$ undergoes a corresponding increase. Quartz content increases downward to a maximum concentration of about 10 per cent near the contact with Sub-unit 2C. Silt layers containing up to 30 per cent foraminifers and as much as 35 per cent sponge spicules, are frequent in the upper part of the sub-unit. These layers range up to 10 cm in thickness and in various cores are characterized by horizontal lamination, cross-lamination, and graded bedding (Figure 8a). In virtually all cases the base of these layers is sharp, whereas commonly they grade upward into marly chalk. Another characteristic is the occurrence of a "halo" of light bluish gray marly chalk surrounding the pinkish gray coarse laminae. In Core 43, where coarse layers are particularly common and are spaced at intervals of 10 to 20 cm, evidence of probably syn-depositional slumping occurs in the form of contorted lamination, pebbles of the surrounding lithology, and pebbles containing nannofossils of Paleocene and Early Cretaceous age (Figure 8b). Maestrichtian foraminifers were observed as contaminants in Cores 44 and 45.

Sub-unit 2C, which extends from 515 to 595 meters, is composed of siliceous mudstones of early-middle Eocene age. They are separated from 2B by a pronounced hiatus which corresponds to upper Eocene time. Notably, carbonate content drops to low values at the level of this hiatus. Siliceous biogenous remains, chiefly sponge spicules but with a significant admixture of radiolarians, reach their maximum concentration in this part of the section. They

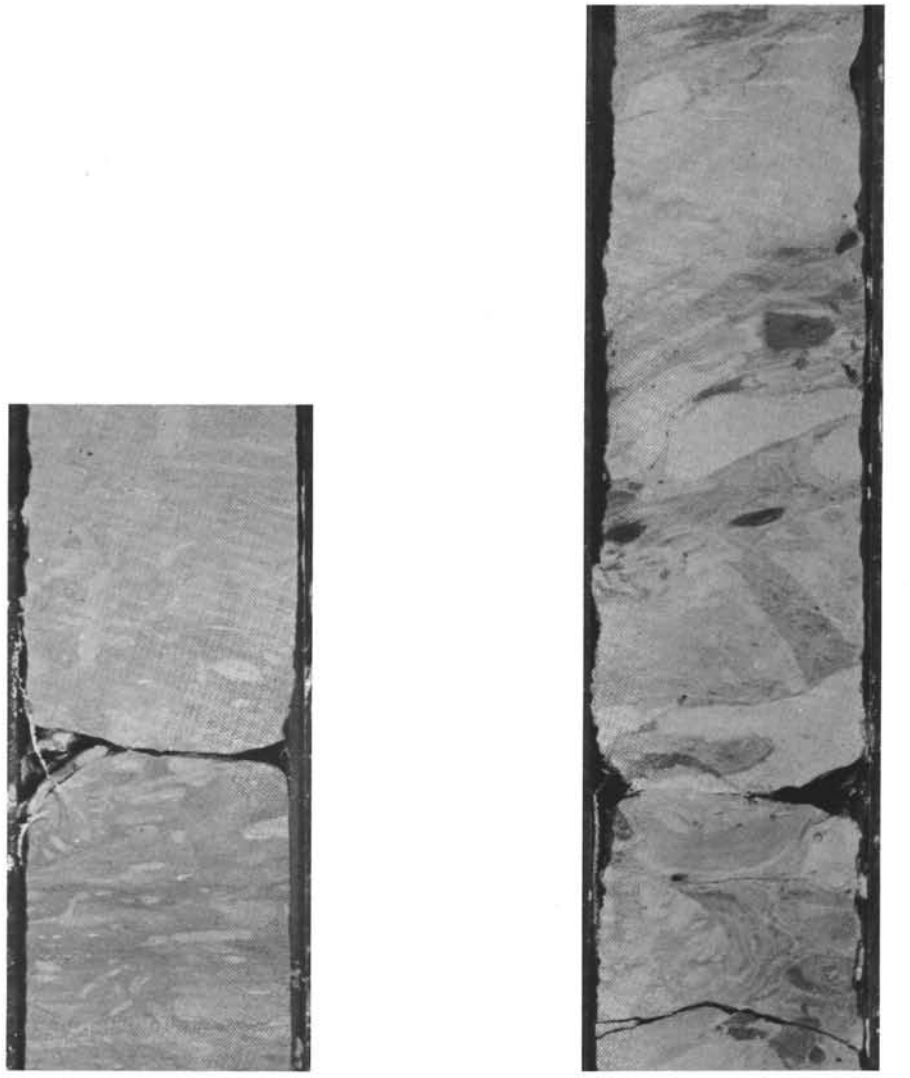

Figure 8. *(a) Lamination in 43-5, 80-95 cm. (b) Slump structures in Sample 43-5, 20-45 cm.*

commonly constitute between 20 and 30 per cent of the sediment and reach peak concentrations of up to 35 per cent in occasional gritty layers. Detrital quartz and clay make up most of the remainder of the sediment. $CaCO_3$ decreases to below 30 per cent in the upper part of the section but becomes progressively more abundant downward so that marly chalks and calcareous mudstone prevail near the bottom of the sub-unit. Accompanying the increase in $CaCO_3$ is a steady decline in detrital quartz content, an increase in zeolite (clinoptilolite), and a pronounced color change. Mudstones in the upper section typically are yellowish gray to olive whereas downward much of the section, in particular the calcareous part, is typified by variegated greenish gray, light brown, and grayish orange. The zeolites generally are most abundant in the oxidized layers. Laminated "gritty" layers of concentrated sponge spicules and occasional evidence of slumping(?) occur throughout the section. A pebble of probable Lower Cretaceous calcareous conglomerate 5 cm in diameter was found at the base of Core 48. Sharp, inclined contacts between contrasting lithologies and occasional offset burrows provide evidence of small-scale faulting.

In Sub-unit 2D corresponding to sub-bottom depths of 590 to 640 meters, relative to the overlying section, carbonate again becomes a dominant constituent due largely to an increase in nannofossils. Although recovery was poor in this interval, evidence indicates that the section consists principally of interbedded yellowish brown marly nannofossil chalk and light greenish gray nannofossil chalk. These range in age from late Paleocene to early Eocene. Accompanying the increase in $CaCO_3$, relative to Sub-unit 2C, is a marked increase in detrital quartz and a decline in siliceous biogenous remains to trace amounts (mainly radiolarians). Foraminifers are conspicuous in the clay-rich layers near the top of the unit.

Mesozoic Units

The Mesozoic section cored at Hole 400A ranges in age from Maestrichtian to late Aptian. The top of the Mesozoic section is defined by an 8-m.y. hiatus between Maestricht-

ian marly nannofossil chalk and upper Paleocene marly nannofossil chalk. Within the Cretaceous, lithologic Units 3 and 4 are separated by the 30-m.y. hiatus between the upper Campanian and the upper Albian (Vraconian).

Unit 3

Recovery in the Upper Cretaceous, as in the Tertiary Section, was poor and the following discussion is on evidence from cavings and the limited core available.

Unit 3 (640-654 m) in the upper part consists of white to bluish white calcareous and marly nannofossil chalks of Maestrichtian age. Cavings in the core suggest that reddish brown and grayish orange-pink chalks may also be present. Slight to moderate bioturbation is present. The chalks are 88 per cent carbonate.

The lower part of the unit, of late Campanian to early Maestrichtian age, is marly nannofossil chalks, reddish yellow in color, with dark brown streaks of organic matter. The color change is reflected by the smear-slide composition which shows a clay content of 55 per cent and a calcium carbonate content of 49 per cent.

The sediments of Unit 3 show a marked increase in the intensity of magnetization over the underlying Lower Cretaceous sediments that may indicate an increased concentration of detrital magnetite. In the clay mineral fraction, smectite is abundant (50%), with subordinate zeolites (30%) and illite (10%).

Unit 3 is separated from Unit 4 by the important 30-m.y. hiatus between the upper Campanian and the upper Albian.

Unit 4

The unit (654-777.5 m) is subdivided into Sub-units 4A and 4B, but is characterized throughout by alternating dark gray to black carbonaceous mudstones and greenish gray calcareous mudstones of late Albian (Vraconian) to late Aptian (Gargasian) age. The sub-units are differentiated on the basis of abundant slumping and higher carbonate content of Sub-unit 4A, and by differences in clay mineral content. Mixed layer illite-smectite is present in 4A but absent in 4B; smectite is less abundant and zeolite is more abundant in 4A than 4B. The lithological boundary between the two occurs at about 711 meters, close to the Albian/Aptian boundary, where the sedimentation rate decreases from about 20 m/m.y. in Aptian time to 7 m/m.y. in Albian time.

Sub-unit 4A (654-711 m) is Albian in age and consists largely of alternating marly nannofossil chalks and carbonaceous marly chalks and mudstones. The upper part of the unit (Cores 62 to Section 3 of Core 64) is characterized by lower quartz (3%), higher carbonate (31-50%), and opal C-T compared to the underlying part of the unit. The change in mineralogy is sharp and occurs in Section 3 of Core 64.

Core 62 (654-663.5 m) contains nine layers of carbonaceous chalks which are typically colored grayish black, are very finely laminated, and range in thickness from 5 to 15 cm. They typically contain 30 to 50 per cent carbonate, 45 per cent clay, and less than 3.3 per cent organic carbon. The intercalated marly nannofossil chalks are dominantly medium bluish gray to light bluish gray but are also mottled medium dark gray. The marly nannofossil chalk contains 30 to 40 per cent carbonate, 35 to 60 per cent clay, and 5 to 10 per cent quartz. Bioturbation is present throughout but is most intense adjacent to the carbonaceous beds.

In Core 63, 16 layers of typically medium dark gray to grayish black carbonaceous chalks are present and range in thickness from 3 to 20 cm. The interbedded marly nannofossil chalks are commonly bioturbated. Within Core 63, abundant evidence of syn-sedimentary deformation is present. Between 47 and 110 cm of Section 4, a typical slump sequence is present and consists of a bottom slip plane, flow structures, microfaulting, slump folding, and flattened clay balls with diameters ranging from 3 to 5 mm (Figure 9). The slumped bed includes carbonaceous marly chalks and is overlain with sharp contact by a carbonaceous mudstone. Microfaulting is also present but appears to be confined to the more competent nannofossil chalks. Zeolites, which may be an alteration product of siliceous organisms, are concentrated in the carbonaceous mudstones.

Seventeen carbonaceous mudstones are present in Core 64 and range in thickness from 5 to 70 cm and color from medium dark gray to grayish black. A well-developed lamination is present and white specks in the mudstone may be zeolites. The intercalated calcareous mudstones are greenish gray and medium bluish gray and commonly are moderately to intensely bioturbated. The carbonaceous mudstone consists of 23 per cent carbonate, 7 per cent quartz, and about 70 per cent clay with the clay fraction consisting of 20 per cent illite, 70 per cent smectite, 1 per cent attapulgite, and 10 per cent clinoptilolite; the organic carbon content is 3.3 per cent. In contrast, the calcareous mudstone contains 25 per cent carbonate, 55 per cent clay, 10 per cent quartz, 5 per cent zeolite, and less than 1 per cent organic carbon.

Between Sections 3 and 5 of Core 64, the interbedded marly nannofossil chalk and carbonaceous mudstones pass downward into interbedded calcareous mudstones and carbonaceous mudstones. The change is associated with an increase in quartz (5-12%) and decrease in carbonate to less than 25 per cent. Organic carbon content in Cores 64 to 67 does not exceed 1.8 per cent. In Core 66, the lowest slump structure is observed.

In Sub-unit 4B the alteration of upper Aptian carbonaceous mudstone and marly nannofossil chalks (711-777.5 m) begins in Core 68 and continues to Core 70. Cores 71 to 74 consist of carbonaceous mudstone and calcareous mudstone. In comparison to Sub-unit 4A, the upper part of Sub-unit 4B is characterized by a higher carbonate content, lower opal C-T and zeolites, and a greater abundance of montmorillonite. Syn-sedimentary deformation is absent.

Core 68 consists of five thin beds of carbonaceous mudstone, typically dark gray to gray-black that exhibit a very fine and well-developed lamination. Two layers of light olive-brown sediment in Sections 2 and 3 are brecciated and contain up to 50 per cent of translucent, mixed layer clay minerals and geothite with subamorphous iron oxides (a comparable lithology is present in Core 70, Section 2). Bioturbation is abundant particularly in the upper part of the interbedded greenish gray to dark greenish gray marly chalk layers. *Zoophycus* burrows are also present.

The same lithologies continue downsection in Cores 71 to 74. Typical thicknesses of the carbonaceous layers are about 10 cm. There is an accompanying decrease in calcium carbonate content and magnesian calcite is observed. The calcareous mudstone contains 20 per cent carbonate, 60 per cent clay, 10 per cent zeolite, 5 per cent quartz, and less than 1 per cent organic matter. In Core 74, pyritic lamina-

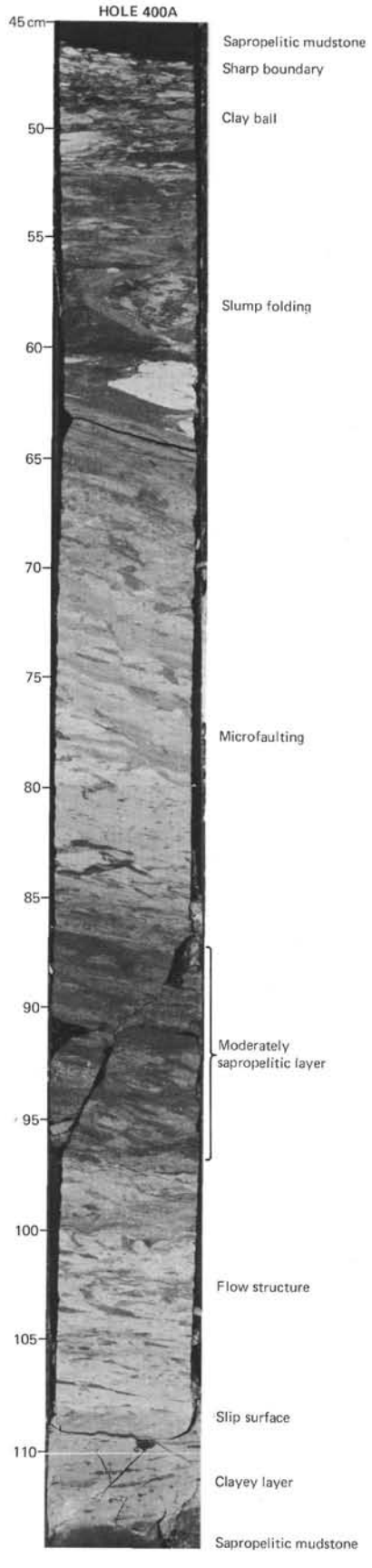

Figure 9. *Slumped structures and microfaulting in Sample 63-4, 40-115 cm.*

tions, sideritic and pyritic concretions, and dolomite are present and may indicate reducing conditions.

GENERALIZATIONS ON THE ALBIAN/APTIAN BLACK SHALE SEQUENCE

A generalized rhythm of the three lithologies observed in the black shale sequence is, from base up, as follows.

Carbonaceous Mudstone

The color ranges from medium dark gray to grayish black and a very fine lamination is prevalent. The lower boundary with the underlying calcareous mudstone generally appears to be gradational, but this may simply be a reflection of the intense bioturbation of the upper parts of the calcareous mudstones. Very fine lamination (<1 mm) is typical though not present in all of the carbonaceous layers. Grading is not apparent although the grain size of the quartz appears largest in this layer. Although specks of zeolite are present, the carbonate content is consistently lower than in the calcareous mudstone.

Silty Claystone

The silty claystone is typically a dark greenish gray homogenous bed that rests with sharp contact on the underlying carbonaceous mudstone but grades upward into the overlying calcareous mudstone. Burrows are rare to absent. The bed may be absent and is indistinguishable, in terms of composition, from the lower part of the calcareous mudstone. The typical silty claystone contains 25 per cent carbonate, 60 per cent clay, 5 per cent quartz, and 3 per cent zeolite.

Calcareous Mudstone

A greenish gray to medium bluish gray color is predominant. Burrowing is moderate to intense in the upper half and slight to moderate in the lower half. Fragments of laminated carbonaceous mudstone are also present.

In these three lithologies, quartz is highest in the carbonaceous mudstone and silty claystone. In contrast, carbonate is least in the carbonaceous mudstone (3%), but increases through the silty claystone (17%) and calcareous mudstone. Zeolites are present in variable quantities (10-60%) throughout all three lithologies but are least in the carbonaceous mudstones. Although grain size determinations are based only on smear slides, a higher proportion of silt-sized material is present in the carbonaceous mudstone 35% (8 values) compared to the silty claystone 7% (7 values) and calcareous mudstone 27% (10 values). A detailed description of the mineralogy of a black shale rhythm is given by Mélières et al. (this volume).

A number of subtle differences exist between the Albian and the Aptian black shale rhythms. In the Aptian, the contrasts between the lithologies are sharp and perhaps accentuated because of lesser bioturbation and the absence of syn-sedimentary deformation. Fragments of carbonaceous mudstone are rare in the Aptian calcareous mudstones but are common in the Albian.

Visual and geochemical determinations suggest a detrital origin for the carbonaceous material. Organic carbon determinations give values of 0.1 to 3.3 per cent by weight. However, shipboard pyrolysis studies show that only 0.1 to

0.3 per cent by weight of pyrolyzable carbon is present, thus indicating a high proportion of carbonized organic matter. In a hydrogen index versus oxygen index diagram, the samples lie on the lowest evolution path characterized by low H and high O content. The low hydrocarbon yields indicate a highly oxidized state for the carbonaceous material prior to deposition and suggest, therefore, detrital supply of carbonized plant remains as the origin for most of the organic matter (see Geochemistry Studies, this volume). The carbonaceous material may have attained its highly oxidized state by chemical or biological degradation very early or it may be the result of reworking.

The alternating lithologic types in both carbonaceous shale units are suggestive of rhythmic sedimentation. Sixty-six rhythms are present in the Albian and 12 in the Aptian.

	Cycle Number	Sedimentation Rate (mm/1000 yr)	Cycle Frequency (1000 yr)
Albian	180-220	7	36-44
Upper Aptian	140	17-23	21-29

Average thickness of units within each rhythm are as follows:

Albian		
	Carbonaceous mudstones	10 cm (66 samples)
	Calcareous mudstones	15 cm (61 samples)
	Silty claystone	5 cm (33 samples)
	Average thickness of rhythm	30 cm
	Average length between carbonaceous mudstones	25 cm
Aptian		
	Carbonaceous mudstones	10 cm (12 samples)
	Calcareous mudstones	30 cm (10 samples)
	Silty claystone	10 cm (5 samples)
	Average thickness of rhythm	50 cm

Thickness and interval data are summarized in Figures 10 and 11, and Table 3.

In comparing the date from the Albian and Aptian, it is clear that the calcareous mudstones and silty claystones are twice as thick in the Aptian as in the Albian where the carbonaceous mudstones remain constant in thickness throughout. These differences can be ascribed only to changes in the sedimentation rate of both terrigenous and carbonaceous material and are discussed in more detail in the Summary and Conclusions.

BIOSTRATIGRAPHY

Upper Quarternary sediments, rich in calcareous microfossils, were recovered from the pilot holes at Sites 399 and 400. Hole 400A was cored continuously from 74.5 to 777.5 meters sub-bottom, penetrating sediments that ranged in age, in an incomplete sequence, from Holocene to Early Cretaceous (Figure 12).

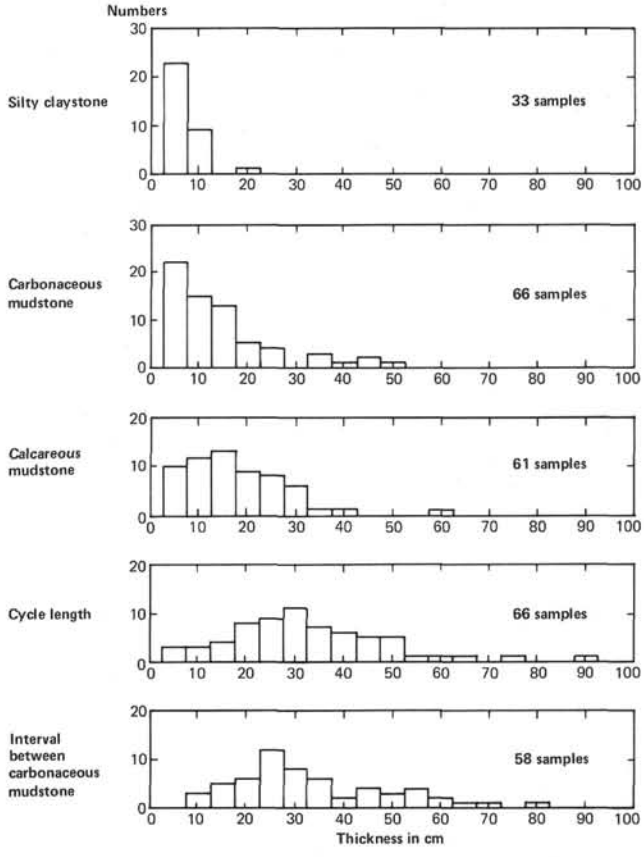

Figure 10. *Thickness and interval of Albian cycles in Hole 400A.*

Carbonate and silica dissolution strongly modified the quality of the paleontological record at this site, in places nearly obliterating it. Sites 399, 400, and Hole 400A must have been near or below the CCD for much of the interval of deposition recorded by these sediments.

The Holocene to lower Pliocene sediments are nannofossil oozes, containing rich foraminiferal and nannofossil assemblages. Both fossil groups reflect oscillations of temperate and subarctic water masses throughout this sequence and the upper Miocene as well.

In lower Pliocene to upper Eocene sediments, the proportion of siliceous microfossil debris within the coarse fraction increases progressively, with a concomitant deterioration of the quality and quantity of calcareous microfossils. It is noteworthy that radiolarians are absent or rare and poorly preserved in this section despite the great abundance of the debris of other siliceous microfossils, mainly sponge spicules. Although apparently complete, the Oligocene sequence is strongly condensed compared with the younger sequences. Below the Oligocene sequence upper Eocene and upper middle Eocene deposits are missing, representing a hiatus of about 7 m.y. Middle Eocene sediments are rich in siliceous microfossils and yielded only a relatively poor record of calcareous microfossils. However, in the lower Eocene and upper Paleocene sediments, carbonate dissolution was less intense and they contain a better preserved record of foraminifers and nannofossils.

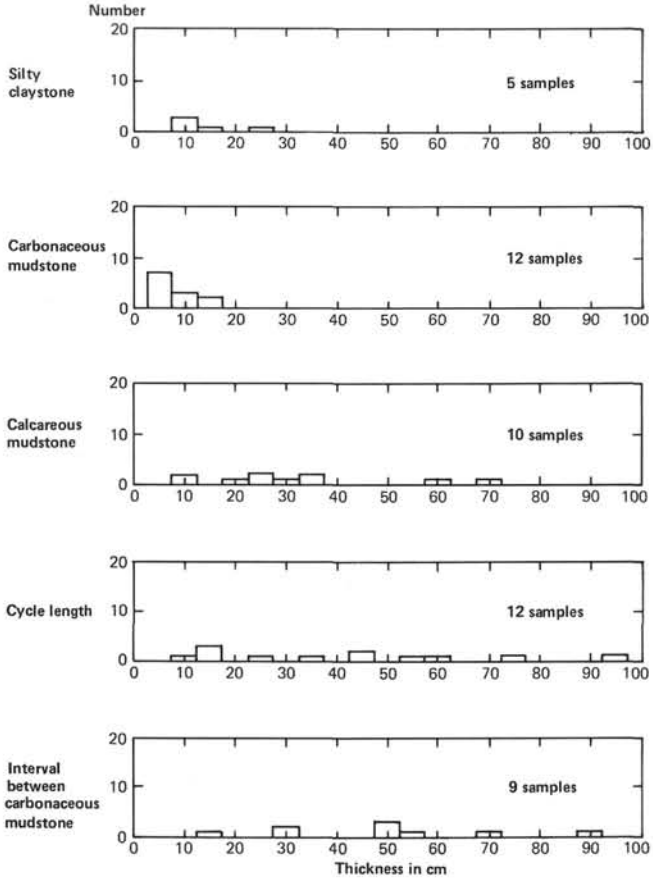

Figure 11. *Thickness and interval of Aptian cycles in Hole 400A.*

TABLE 3
Rhythm Frequency

	Core	Thickness	Time Interval (m.y.)	Cycle Length (cm)
Albian	62-67	55	8	25-30
Upper Aptian	68-74	70	3-4	50

Middle and lower Paleocene and upper Maestrichtian sediments are absent; a hiatus of approximately 9 m.y. separates the oldest Tertiary sediments from the youngest Cretaceous sediments. A short section of lower Maestrichtian and upper Campanian sediments, consisting of white chalk and red marls, contains only a poorly preserved nannofossil flora and a few benthic but no planktonic foraminifers. This Late Cretaceous sequence is separated from the underlying Early Cretaceous sequence by a hiatus of about 22 m.y.

Cyclic sequences of black shales and lighter colored marls of Albian and late Aptian age contain calcareous microfossils which are rare and poorly preserved within the black shale layers, but moderately to well preserved, though not abundant, within the gray layers. Wherever calcareous microfossils are scarce, siliceous microfossil debris is abundant, suggesting cycles of varying rates of carbonate dissolution. Radiolarians are present in highly variable abundances and mostly poorly preserved.

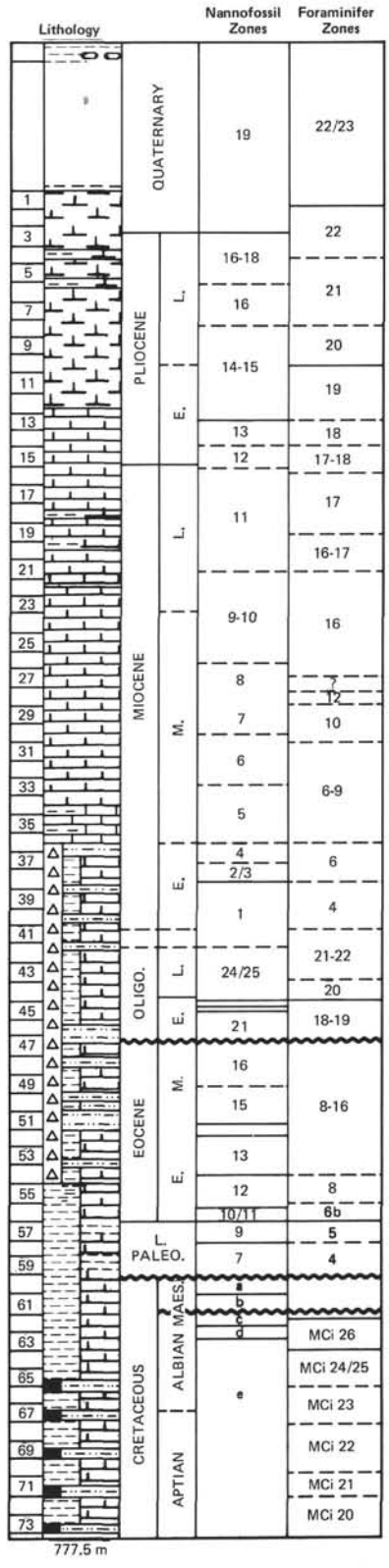

Figure 12. *Generalized biostratigraphic zonation of sediments in Holes 400/400A. Mesozoic nannofossil zones are:* (a) Lithraphidites quadratus *Zone,* (b) Tetralithus trifidus *Zone,* (c) Eiffellithus turriseiffeli *Zone,* (d) Prediscosphaera cretacea *Zone,* (e) Parhabdolithus angustus *Zone. See text for detailed discussion.*

Reworked nannofossils were encountered frequently but could be recognized easily as such and posed no stratigraphic problem. Reworked foraminifers occurred only rarely. No purely allochthonous deposits, or evidence of slumping, were encountered at these sites. The benthic foraminifers of the Tertiary and Upper Cretaceous deposits were all indicative of abyssal depth, whereas a few well preserved species of possible shallow water origin were found in the Aptian and Albian sequence. Hole 400A has probably been at bathyal depth throughout the time interval represented by the sediments encountered.

Foraminifers

Holocene sediments recovered in Core 1 of both Sites 399 and 400, contained a planktonic foraminiferal fauna that was dominated by *Globorotalia inflata* and *Globigerina bulloides*. Such a fauna is typical of the transition zone (Bé and Tolderlund, 1971). Pleistocene sediments at Sites 399, 400 and Hole 400A contained alternating layers bearing either a fauna similar to the Holocene fauna or one dominated by *Globigerina pachyderma* and, to a lesser extent, by *G. bulloides*, a fauna termed subarctic by Bé and Tolderlund. These alternations clearly document the oscillations of contrasting water masses at the sites in response to the worldwide climatic fluctuations. These cycles continued downhole, but with diminished contrast, to the upper Miocene section. Benthic foraminifers responded as well to the glacial-interglacial oceanographic contrast; their abundance rose from less than 1 per cent of all foraminifers during interglacial stages to more than 3 per cent during glacial stages, and the composition of the fauna changed from a dominance of *Oridorsalis umbonatus, Epistominella exigua, Melonis pompilioides, Planulina wuellerstorfi,* and others during interglacials, to a dominance of *Uvigerina peregrina, Uvigerina asperula,* and *Globocassidulina subglobosa* during glacials. Although this glacial bottom fauna presently resides nearly 2000 meters higher, on the continental slope, these changes in the benthic foraminiferal faunas should not be interpreted in terms of depth changes but rather in terms of climatically controlled changes of the abyssal thermohaline circulation (Streeter, 1973; Schnitker, 1974).

The Pleistocene/Pliocene boundary, defined here by the *Globorotalia tosaensis-Globorotalia truncatulinoides* transition, occurred at 108 meters sub-bottom (Core 4, Section 4). Lower Pliocene is indicated by the occurrence of *Globorotalia acostaensis* in Sample 10-1, 57-59 cm.

The Pliocene-Miocene boundary probably lies within Core 15, where the lowest but somewhat questionable *Globorotalia margaritae* were found. The upper Miocene section extends down to approximately 330 to 340 meters sub-bottom (Core 27 or 28). Within this interval, calcium carbonate dissolution becomes progressively more severe; planktonic foraminiferal faunas are poorly preserved and often of low diversity. Index species are commonly absent. The precise boundaries between Zones N.18 and N.17 and between N.17 and N.16 could not be determined. The fauna of Core 29, which probably contained the late to early Miocene boundary, could not be dated better than belonging to Zones N.15 to N.16. Sample 29-1, 114-116 cm, is of middle Miocene age (N.10 to N.12). It is possible that a hiatus of one to two million years exists near the mid to late Miocene boundary. The mid to early Miocene boundary could not be determined. Samples from Cores 33, 34, 35, and the top of Core 36 never yielded more than three to four poorly preserved species of planktonic foraminifers which gives only a broad age assignment of Zones N.6 to N.9. Sample 36-1, 42-45 cm contained *Catapsydrax dissimilis*, confirming that the lower Miocene had been reached. Zone N.5 was not encountered, indicating the possibility of a 3-m.y. hiatus between Samples 38, CC and 39-1, 117-118 cm. Two lower Miocene samples (39-1, 117-118 cm and 39, CC) contain reworked Oligocene species (*Globorotalia increbescens* and *Globigerina ampliapertura*) which are better preserved than the autochthonous fauna.

The Miocene-Oligocene boundary lies probably within Core 41 or 42. The sample above (40, CC) is still of early Miocene age, and the sample below (43-2, 65-67 cm) is of late Oligocene age (Zones P.21 to P.20). The late/early Oligocene boundary falls between Samples 45, CC and 46-4, 41-43 cm.

A hiatus of about 7 m.y. lies between Sample 47-1, 21-24 cm of early Oligocene age (P.18) and Sample 47, CC of middle Eocene age (P.12). Sample 47-6, 99-101 cm contained pyritized radiolarians and sponge spicules and clasts with manganese crusts, but no foraminifers. Within the middle and the upper lower Eocene sediments, foraminiferal preservation is commonly too poor to permit resolution of all foraminiferal zones which appear to be present.

The Eocene/Paleocene boundary, the boundary between Zones P.6a and P.6b, occurs in Sample 57-2, 4-7 cm. Below, upper Paleocene sediments (Zones P.6a to P.4) contain abundant and excellently preserved planktonic and benthic foraminifers.

The Tertiary/Mesozoic boundary lies between Cores 59 and 60. Age determinations for the Upper Cretaceous sediments are based solely on nannofossils; they are barren of planktonic foraminifers. The benthic foraminiferal species are not age diagnostic, but are compatible with the early Maestrichtian and late Campanian nannofossil age determinations. The hiatus between the Maestrichtian and Paleocene sediments was of about 9 m.y. duration. A urther hiatus of about 30 m.y. lies between Samples 61, CC and 62-1, 70-73 cm.

Uppermost Albian (Vraconian) sediments are recovered in Sample 62-1, 70-73 cm, corresponding to the *Rotalipora appenninica/Planomalina buxtorfi* Zone (MCi 27). From Samples 62-2, 28-30 cm to 63-4, 28-30 cm, *Rotalipora ticinensis, Ticinella breggiensis,* and *Ticinella raynaudi digitalis* indicate the *Ticinella breggiensis* Zone (MCi 26) of late Albian age. The fauna in Core 63 is composed of small specimens only and contained abundant radiolarians. Small and poorly preserved *Hedbergella planispira* are present from Core 64, Section 1 to Core 66, Section 1 suggesting a middle Albian to late early Albian age *(Hedbergella rischi/ Ticinella primula* Zone (MCi 25) to *Hedbergella planispira* Zone (MCi 24).

Ticinella bejaouaensis, defining the *T. bejaouaensis* Zone (MCi 23) of the early early Albian and latest Aptian, is present from Samples 66-2, 63-67 cm downwards to 68-1, 95-97 cm. The Aptian/Albian boundary between Core 68,

Section 1 and Core 67 is based upon the occurrence of *Pleurostomella subnodosa* above that level.

The late Aptian (Gargasian) *Hedbergella trocoidea* Zone (MCi 22) is present between Samples 68-2, 111-113 cm and 70, CC. *Hedbergella trocoidea* is often abundant and of relatively large size in this sequence.

The *Globigerinelloides algerianus* Zone (MCi 21) (late Aptian-Gargasian) is reached in Core 71. Downcore, planktonic foraminifers became scarce and finally disappear, so that further age assignments cannot be made. "Primitive" agglutinated foraminifers remain present in the samples as well as some radiolarians.

Nannofossils

Pleistocene sediments of the *Emiliania huxleyi* Zone (NN 21) and *Gephyrocapsa oceanica* Zone (NN 20) were recovered in Cores 1 and 2 at Site 399 and in Core 1 at Site 400. Some samples are poor in autochthonous nannofossils because of dilution with terrigenous material, but the samples are distinguished by the abundance of reworked Cretaceous and Eocene species.

The Pleistocene nannoplankton assemblage belongs to the transitional zone with the following species: *Emiliania huxleyi, Coccolithus pelagicus, Cyclococcolithus leptoporus, Helicosphaera carteri, Syracosphaera pulchra, Gephyrocapsa* sp. (probably a small variety of *G. oceanica),* and a few specimens of *Scapholithus fossilis, Rhabdosphaera clavigera,* and *Umbilicosphaera mirabilis.*

Intercalated white layers of nannofossil ooze consist mainly of *Gephyrocapsa* sp. and *Coccolithus pelagicus.* They may indicate an influx of northern cold water masses. The *Pseudoemiliania lacunosa* Zone (NN 19) is determined from Core 1 to Sample 3-2, 100-101 cm (−74.5 to −95.0 m) in Hole 400A. The abundance of *Discolithina japonica* and *Pontosphaera pacifica* in the *Pseudoemiliania lacunosa* Zone (NN 19) is remarkable.

The Pliocene/Pleistocene boundary in Hole 400A is determined by the extinction of *Cyclococcolithus macintyrei,* because discoasters are missing in the upper Pliocene sequence. Paleomagnetic measurements have shown that this biostratigraphic horizon lies near the top of the Olduvai event, which corresponds well with the extinction level of *Discoaster brouweri. Coccolithus pelagicus, Cyclococcolithus macintyrei, Pseudoemiliania lacunosa,* and *Cyclococcolithus leptoporus* are the most frequent species of the upper Pliocene sediments, whereas discoasters are missing or occur only sporadically. The sediments of this sequence are rich in slightly etched nannofossils. Some layers are marked by a higher amount of terrigenous material and reworked species from the Cretaceous, indicating that the first ice-rafted material occurred already in the late Pliocene, approximately within the upper part of the *Discoaster surculus* Zone (NN 16) at about 3 to 2.7 m.y.

The subdivision of the upper Pliocene is difficult because discoasters are missing. The last discoasters occur within the *Discoaster surculus* Zone (NN 16) where they are present only sporadically (Sample 6-2, 100-101 cm). The base of the *Discoaster surculus* Zone (NN 16) is determined in Sample 8-1, 100-101 cm (at −142.0 m). The sediments of this zone are rich in well-preserved nannofossils.

The lower Pliocene is present from Samples 8-2, 90-91 cm to 15-5, 23-24 cm. The zone boundaries are not precise because of the absence or scarcity of index fossils. The stratigraphic interval which corresponds to the *Discoaster asymmetricus/Reticulofenestra pseudoumbilica* Zone (NN 14/NN 15) is determined from Samples 8-2, 90-91 cm to 13-4, 96-97 cm. The determination of the boundary between these two zones is not possible because *Ceratolithus tricorniculatus* is absent. Well-preserved nannofossils are abundant in this sequence. *Ceratolithus rugosus* occurs only in few samples. *Reticulofenestra pseudoumbilica* is smaller in the upper part of the nannoplankton Zone NN 15 where a short overlapping of *R. pseudoumbilica* and *Pseudoemiliania lacunosa* can be observed.

The interval of the *Ceratolithus tricorniculatus/ Ceratolithus rugosus* Zone (NN 12/NN 13) is recovered from Samples 13-5, 73-74 cm to 15-5, 23-24 cm. A subdivision is not possible because *C. rugosus* was not found. The sediments are rich in well-preserved nannofossils. Slightly warmer surface water temperatures during the early Pliocene are indicated by the presence of discoasters.

The *Discoaster quinqueramus* Zone (NN 11) of the upper Miocene is determined from Samples 16-1, 87-88 cm to 21, CC (−218.0 to −274.0 m). This determination is based mainly on the presence of *Ceratolithus tricorniculatus* together with *Discoaster calcaris; Discoaster quinqueramus* is restricted to only a few samples. Fluctuations of water temperatures can be assumed by the variable abundance of discoasters. *Ceratolithus tricorniculatus* is present in samples in which discoasters are abundant, whereas it is scarce or missing in layers with only few discoasters. Concurrent fluctuations of the CCD are observed. In general, a correlation exists between layers rich in discoasters and less etched nannofossils (lower level of the CCD) indicating warmer water temperatures, and layers which are poor in discoasters with strongly etched and broken nannofossils (higher level of the CCD), indicating lower water temperatures.

The nannofossils of the *Discoaster quinqueramus* Zone (NN 11) are abundant, but are strongly etched and broken in some layers, whereas they are well preserved in others. *Discoaster quinqueramus* and *D. pentaradiatus* are almost restricted to the upper part of this zone which may indicate a slight warming during the latest Miocene. *Sphenolithus abies* is missing or scarce.

Core 22 to Core 26 belong to the stratigraphic interval of the *Discoaster hamatus/Discoaster calcaris* Zone (NN 9/NN 10). An unequivocal determination of the *Discoaster hamatus* Zone (NN 9) is not possible because the index species *D. hamatus* and *D. bollii* are missing, probably caused by low water temperatures. This does not, however, imply that Zone NN 9 is not represented. *Discoaster calcaris, D. brouweri,* and *D. variabilis* are common in several samples. Few specimens similar to *D. exilis* have been observed.

The sporadic occurrence of *Catinaster coalitus* in Core 27, Section 1 indicates the *Catinaster coalitus* Zone (NN 8) of the middle Miocene. Cores 29 and 30 belong to the *Discoaster kugleri* Zone (NN 7) with *D. kugleri, D. exilis,* and a great variety of *Coccolithus pelagicus (=C. miopelagicus).*

The *Discoaster exilis* Zone (NN 6) is present in Cores 31 and 32. *Discoaster exilis* is abundant, whereas *Coccolithus abisectus* is scarce. Few specimens of *Sphenolithus heteromorphus* are present within the nannoplankton Zones NN 6 and NN 7. Sediments of the middle Miocene sequence are rich in nannofossils of variable preservation which shows fluctuations of the CCD. Reworked species from the Eocene occur sporadically in some samples.

The *Sphenolithus heteromorphus* Zone (NN 5) is determined from Samples 34, CC to 36, CC. Nannofossils are abundant, coccoliths are strongly etched and broken, discoasters are overgrown. *Coccolithus abisectus, C. pelagicus, Discoaster exilis, Reticulofenestra pseudoumbilica,* and *Sphenolithus heteromorphus* are the most abundant species.

The sequence from Samples 37-1, 48-49 cm to 37-4, 14-15 cm probably belongs to the *Helicosphaera ampliaperta* Zone (NN 4) of the lower Miocene. However, *H. ampliaperta* and *Sphenolithus heteromorphus* were not observed. If the determination of the nannoplankton Zone NN 4 is correct, it can be suggested that *S. heteromorphus* in high latitudes does not occur earlier than within the nannoplankton Zone NN 5. *Sphenolithus belemnos* was found from Sample 37, CC to 38, CC indicating the *Discoaster druggii/Sphenolithus belemnos* Zone (NN 2/ NN 3) of the lower Miocene. Subdivision of the two zones is not possible.

Cores 39 to 42 (−435.5 to −473.5 m) probably belong to the lowermost Miocene; exact determination is not possible. The nannofossils are small, and sponge spicules and diatoms are more frequent than above. Upper Eocene sediments were found in Sample 41-1, 16-17 cm, probably brought in by slumping.

The determination of the Oligocene/Miocene boundary between Cores 42 and 43 is uncertain. It is based on the extinction of *Dictyococcites dictyodus,* because *Helicosphaera recta* and sphenoliths are missing.

A complete Oligocene sequence is determined from Sample 43-1, 1-2 cm to 47-1, 79-80 cm. The sediments contain abundant but badly preserved nannofossils.

Samples 43-1, 1-2 cm to 45-3, 56-57 cm belong to the *Sphenolithus distentus/Sphenolithus ciperoensis* Zone (NP 24/NP 25) of late middle Oligocene and the late Oligocene age. The scarcity of sphenoliths in these samples is probably due to ecological factors, particularly in view of their complete absence from all Rockall Bank sites. The *Sphenolithus predistentus* Zone (NP 23) is determined by the absence of *Coccolithus abisectus* and the presence of few specimens of *Spenolithus predistentus* and *S. distentus* from Samples 45-3, 113-114 cm to 45-5, 81-82 cm. Strongly etched nannofossils are numerous.

Samples 45, CC to 47-1, 79-80 cm are early Oligocene in age: Sample 45, CC contains the *Helicosphaera reticulata* Zone (NP 22), Samples 46-3, 105-106 cm and 47-1, 79-80 cm contain the *Ericsonia subdisticha* Zone (NP 21). Nannofossils are abundant, strongly etched, and broken. Few specimens of *Chiasmolithus oamaruensis* occur in the lower Oligocene sediments. Their occurrence in this stratigraphic interval is known from regions of low water temperatures.

A hiatus, which represents an interval of about 7 m.y., lies between Samples 47-1, 79-80 cm and 47-6, 143-146 cm. The lower Oligocene is underlain by the middle Eocene sequence. Samples 47-6, 143-146 cm to 52-1, 9-10 cm belong to the *Discoaster tani nodifer/Chiphragmalithus alatus* Zone (NP 15/NP 16). Subdivision of the two zones by the extinction of *Rhabdosphaera gladius* is impossible, because the species is missing. The last occurrence of *C. alatus* was observed in Sample 49-2, 20-21 cm. The sediments of this interval contain numerous siliceous microfossils, nannofossils having been dissolved and/or diluted by the high amount of siliceous microfossils. In some samples discoasters are enriched by selective dissolution of the more fragile coccoliths.

The *Discoaster sublodoensis* Zone (NP 14) of the middle Eocene is determined from Samples 52-1, 108-109 cm to 53-1, 11-12 cm. *Discoaster sublodoensis, D. barbadiensis,* and *D. distinctus* are abundant, whereas *D. nonaradiatus* and *D. lodoensis* are scarce.

The *Discoaster lodoensis* Zone (NP 13) is determined from Samples 53-1, 146-147 cm to 54, CC with abundant *Discoaster lodoensis* but without *D. sublodoensis*. Siliceous microfossils are absent from Sample 54-3, 25-26 cm downwards. There are many nannofossils; coccoliths are strongly etched whereas the discoasters are enriched by selective dissolution.

Samples 55-1, 103-104 cm to 56-2, 61-62 cm belong to the *Marthasterites tribrachiatus* Zone (NP 12); Sample 56, CC to the *Discoaster binodosus* Zone (NP 11); and Sample 57-1, 148-149 cm to the *Marthasterites contortus* Zone (NP 10). Nannofossils are abundant in this sequence. Coccoliths are strongly etched, whereas the discoasters are slightly overgrown.

Upper Paleocene sediments are recovered from Sample 57, CC to 59, CC. Samples 57, CC and 58, CC belong to the *Discoaster multiradiatus* Zone (NP 9). Well-preserved nannofossils are abundant and a few reworked species from the Cretaceous are present. Samples 59-1, 25-26 cm to 59, CC belong to the *Heliolithus riedeli* Zone (NP 8).

The Cretaceous/Tertiary boundary lies between Cores 59 and 60. The uppermost Maestrichtian *(Tetralithus murus* Zone) is not represented. The thickness of the Upper Cretaceous sequence is extremely reduced. The *Lithraphidites quadratus* Zone of the Maestrichtian is determined in Sample 60, CC; the *Tetralithus trifidus* Zone of late Campanian/earliest Maestrichtian age in Sample 61, CC. Nannofossils are very abundant, but they are almost all completely broken.

A hiatus of about 22 m.y. lies between Samples 61, CC and 62-1, 61-62 cm.

The *Eiffellithus turriseiffeli* Zone of late Albian/early Cenomanian age is determined from Samples 62-1, 61-62 cm to 63-1, 41-42 cm and the *Prediscosphaera cretacea* zone of the middle Albian from Samples 63-2, 4-5 cm to 65-1, 39-40 cm. *Eiffellithus turriseiffeli* and *Prediscosphaera cretacea* are small and are scarce in this sequence

The *Parhabdolithus angustus* Zone of late Aptian/early Albian age is present from Samples 65-2, 23-24 cm to 74, CC. Sediments contain many well preserved to strongly etched nannofossils, they being more strongly etched within the dark layers than in the gray marls. Nannoconids occur only sporadically in some samples. Species of the genus *Parhabdolithus* are the most frequent.

The Aptian/Albian boundary is determined with the first occurrence of *Hayesites albiensis* in Sample 68, CC. This boundary corresponds well with the Aptian/Albian boundary on the basis of foraminifers and dinoflagellates.

Dinoflagellates[2]

Site 399

From the limited (11.77 m) core recovered from Site 399, two samples (399-1-4, 60-62 cm and 399-1-4, 62-64 cm) were processed. Both samples yielded sparse assemblages of well-preserved dinoflagellates dominated by peridiniacean cysts such as *Brigantedinium cariacoensis* (Wall) Reid, *B. simplex* (Wall) Reid, *Multispinulosa quanta* Bradford, and *Trinovantedinium capitatum* Reid. Other species in the assemblages include *Bitectatodinium tepikiense* Wilson, *Operculodinium centrocarpum* (Deflandre and Cookson) Wall, and *Umrindeta* sp. indet. These assemblages are similar in composition and in their proportions to the "Southern North Sea" assemblage of Reid and Harland (in press) and suggest a Devensian or early Flandrian assignment. The dinoflagellate cyst evidence appears to support a southern shift of the North Atlantic water circulation pattern, in comparison to the present-day situation, with the "Southern North Sea" assemblage occupying an area where it is not normally recovered. The Recent dinoflagellate cyst assemblage for the area is discussed in the notes for Site 400. Evidence of contamination and reworking was not observed, and terrigenous palynomorphs and organic debris form minor elements in the assemblages.

Site 400

Initially a single sample from Site 400 (400-1-1, 90-92 cm) was investigated and proved a sparse, non-diagnostic assemblage of dinoflagellate cyses. Thirteen additional samples of Quaternary sediments were processed and are fully discussed in the main report on dinoflagellate palynostratigraphy of the Cenozoic from the Bay of Biscay. These samples, indicative of a Devensian and Flandrian assignment, yield information on the late Quaternary history of the circulation of the North Atlantic in relation to changing climates, and in particular have substantiated a southern shift, in relation to the present situation, of the "Southern North Sea" assemblage of Reid and Harland (in press) into the Biscay area. This area at present is characterized by an "East Atlantic" assemblage, which contains a predominance of *Spiniferites* spp. including *S. mirabilis* (Rossignol) Sarjeant together with significant proportions of *Operculodinium centrocarpum* (Deflandre and Cookson) Wall, and *Nematosphaeropsis labyrinthea* (Ostenfeld) Reid as seen in Samples 400-1-1, 40-42 cm and 400-1-1, 110-112 cm. This alteration in the oceanic circulation pattern probably correlates with a deterioration of climate in the Northern Hemisphere. Little or no contamination and reworking was noted, and the influence of terrigenous palynomorphs and organic debris is minor.

Hole 400A

Initial samples from the core at Hole 400A produced an excellent sequence of well-preserved middle Miocene to Pleistocene dinoflagellate cysts that have allowed a tentative fourfold biostratigraphic zonation to be erected. The uphole appearance of stratigraphically important species is seen in Sample 400A-26-3, 49-53 cm, where *Amiculosphaera umbracula* Harland, *Bitectatodinium tepikiense* Wilson, and *Leptodinium aculeatum* Wall are first recorded; in Sample 400A-13-3, 111-113 cm, where *Spiniferites mirabilis* (Rossignol) Sarjeant, *S.* cf. *pseudofurcatus* (Klumpp) Sarjeant, and *Tectatodinium pellitum* Wall appear and, finally, in Sample 400A-1-3, 110-114 cm, where *Spiniferites elongatus* Reid and *Trinovantedinium capitatum* Reid are first recorded. Although the dinoflagellate cysts cannot in themselves be used to date the sediments recorded from Hole 400A, calcareous micropaleontological evidence suggests the first mentioned species occur in the middle Miocene, NN 8 to NN 10, the second in the early Pliocene at the NN 13/14 boundary, and the last mentioned in the Pleistocene, within NN 19. A full account of this biostratigraphy is presented elsewhere in this volume.

Although sporadic barren samples do occur above Sample 35-3, 93-95 cm (Sample 22-3, 65-67 cm and 39-1, 80-84 cm), at this horizon the remaining downhole samples of Tertiary sediment mostly prove to be barren of dinoflagellate cysts. One or two exceptions, however, did occur, but contained only sparse dinoflagellate assemblages (Sample 37-3, 67-70 cm; 39-1, 90-92 cm; 40-1, 20-22 cm; and 47-4, 103-107 cm). Only the last-mentioned sample yields age-diagnostic species and, in particular, *Samlandia chlamdophora* Cookson and Eisenack which has a known range of early Eocene to early Oligocene in Europe (Harker and Sarjeant, 1975). The nannofossil and planktonic foraminiferal evidence from this core indicates a middle Eocene age.

Thirty-six additional samples of lower Pleistocene and upper Pliocene sediments were also examined in detail and have indicated certain aspects relating to the history of the North Atlantic circulation and have offered some evidence on the phylogeny of dinoflagellates. The potential of using such species as *Amiculosphaera umbracula* Harland, *Operculodinium crassum* Harland, and *Spiniferites rubinus* (Rossignol) Sarjeant in recognizing the lower Pleistocene/Pliocene appear to be particularly valuable. A full account of the Quaternary dinoflagellate palynostratigraphy occurs elsewhere in this volume. No contamination reworking was noted in samples from Hole 400A, and terrigenous palynomorphs and organic debris were a minor constituent.

Marine Aptian/Albian Palynology of Hole 400A[3]

All of the Aptian/Albian samples examined from Samples 62-2, 41-43 cm to 74-1, 4-6 cm yielded relatively rich and diverse dinocyst assemblages. Sporomorphs are abundant, usually making up more than 50 per cent of the palyno-

[2]Contribution by Rex Harland, Institute of Geological Sciences, Ring Road Halton, Leeds, England.

[3]Contribution by R. J. Davey, Institute of Geological Sciences, Ring Road, Halton, Leeds, England.

morph assemblage, and consist mainly of bisaccate pollen grains; spores are rare. Microforaminifers and acritarchs are rare or absent. Preservation is good in all cases, and no reworking is recognized.

Dating was done by comparing dinocyst ranges at this site with known ranges in accurately dated onshore sections in southern England and northern France. Details are to be found elsewhere in this volume (Davey), and the following is only a summary.

Sample 62-2, 41-42 cm contains *Litosphaeridium siphoniphorum* and *L. conispinum* which together are indicative of the upper *M. inflatum* Zone of the upper Albian. Sample 62-4, 111-113 cm contains the youngest stratigraphic occurrence of *L. arundum* and Sample 63-2, 80-83 cm contains the earliest stratigraphic occurrences of *Apteodinium grande, Hexagonifera chlamydata,* and *L. conispinum*. These distributions all indicate that these two samples belong to the *M. inflatum* Zone. *Systematophora cretacea* occurs in Samples 64-3, 52-55 cm; 65-2, 19-22 cm; and 66-3, 55-60 cm; and, although it has been recorded from the *D. cristatum* Zone (upper Albian), it is normally restricted to the middle Albian.

Several species have their topmost stratigraphic occurrences in Section 67-0 and Sample 68-2, 24-26 cm and have not been recorded from the Albian; these include *Cyclonephelium tabulatum, Muderongia* cf. *staurota, Polystephanephorus anthophorum, Subtilisphaera perlucida,* and *Surculosphaeridium trunculum*. These samples are hence assigned an Aptian age and the Aptian/Albian boundary is placed above the younger sample. The presence of *Meiourogonyaulax stoveri* and *Cauca parva* in Section 70-0 and *Chlamydophorella huguonioti* in Sample 72-3, 40-42 cm indicates that the early-late Aptian boundary should be placed between these two samples.

The samples analyzed consist either of marly nannofossil chalk or sapropelic mudstone and each yields characteristic palynologic assemblages. Firstly, the chalk and sapropelic mudstone differ in that the organic debris in the chalk consists almost entirely of carbonized tracheidal material whereas in the mudstone this is a minor element and noncarbonized, terrestrially derived tracheidal and cuticular material is abundant. Secondly, in the chalk the dinocysts make up between 14 and 77 per cent (average 47%) of the palynomorph assemblage whereas, in contrast, the dinocysts in the mudstones make up only 10 to 18 per cent (average 14%) of the assemblage. Spores are consistently rare (<1-6%), and the remainder of the assemblage consists of bisaccate pollen grains (21-87%). This unusually high abundance of bisaccates, particularly over spores, strongly suggests that the site deposition was at some distance from the landmass.

At the time of chalk deposition, sedimentation was slow and nearshore characteristics are absent. During sapropelic mudstone deposition at Hole 400A, the landmass had a strong influence, and the organic content of the samples closely resembles that obtained from the Aptian/Albian of Hole 402A. However, at Hole 400A, generally nearshore and shelf constituents, such as microforaminifers, are almost absent and the peridinacean dinocysts, particularly the genera *Ovoidinium* and *Subtilisphaera,* are only minor constituents, whereas at Hole 402A these are often present and abundant. Such characteristics again indicate that the Aptian/Albian at Hole 400A was deposited at a reasonable distance from the landmass and probably not on the continental shelf.

PHYSICAL PROPERTIES

Determinations of the physical properties of sediments from Sites 399 and 400 involved 129 samples from 844 meters of cored section, of which 777.5 meters were from Site 400, for an average of one sample per 6.5 meters of hole. Loss of the drill string prevented downhole logging. The introduction to this volume includes a brief discussion of purpose and procedures for these measurements and related calculations.

The ranges of determinations include: coring time (0.6-12.7 min/m), sound speed (1.5-1.95 km/s), wet bulk density (1.4-2.07 g/cm^2), sound impedance (2.3-3.84 units), porosity (37-74%), water content 17-47% wt.). The data are presented in Tables 4 and 5 and depth plots for Site 400 only are shown on the superlog enclosed in the pocket of this volume.

Recognizable trends in one or more physical property occur within four sub-bottom depth intervals indicated in meters. These reasonably reflect composition and compaction (0-200), compaction only (200-370), onset of cementation (370-445), and mostly composition (445-755). From 0 to 200 (discounting some large fluctuations of wet bulk density and therefore sound impedance as data scatter) the trend shows linear increases in coring rate, sound speed, and wet bulk density together with linear decreases in porosity and water content, all qualitatively explainable by compaction and/or the linear increase in per cent $CaCO_3$ (40-75%). The interval from 200 to 370 meters sub-bottom likewise shows linear increases of coring rate, sound speed, and wet bulk density with decreases in porosity and water content; the $CaCO_3$ content remains constant at 85 per cent, suggesting compaction.

The interval between 370 and 445 meters sub-bottom probably causes a prominent seismic reflector, apparently related to cementation. In contrast to the overlying sediments, the greater rates of increase of both sound speed and wet bulk density, when multiplied together, produce an abrupt increase in sound impedance with a maximum between 410 and 420 meters. The interval from 370 to 408 meters includes the onset of sound speed anisotropy (0-6%) and greater rate of sound speed increase where wet bulk density continues to increase consistently with decreases in porosity and water content, but where the percent $CaCO_3$ decreases. The continued slight increase in sound speed from a depth 408 to 445 meters seems to parallel a slight decrease in wet bulk density.

Fluctuations of physical properties in the interval from 445 to 755 meters generally parallel the per cent $CaCO_3$ including several prominent impedance changes that reasonably mark seismic reflectors at meter depths of approximately 480, 555, and 585 meters. Discrepancies to this generalization at depths of 508, 580 to 600, and 650 meters may reflect variable combinations of compaction and cementation as well as composition (i.e., if the elastic properties of the sediment remain constant, the sound speed varies inversely with wet bulk density). For example, the

TABLE 4
Physical Property Summary, Site 399

Sample (Interval in cm)	Depth Sub-Bottom (m)	Strength Vane Shear (g/cm^2) Original	Strength Vane Shear (g/cm^2) Re-Mold	Sound Velocity (km/s) Hamilton Frame ∥ to Beds	Sound Velocity (km/s) Hamilton Frame ⊥ to Beds	Anisotropy ∥-⊥	Anisotropy ∥-⊥ / ⊥ (%)	C°	Wet Bulk Density (g/cm^2) GRAPE 2 Minute ∥ Beds	GRAPE 2 Minute ⊥ Beds	Syringe (wt./vol.)	Chunk (wt./vol.)	Sound Impedance $\left[\frac{g}{(cm^2/s)}\right] 10^5$ GRAPE Density	Sound Impedance $\left[\frac{g}{(cm^2/s)}\right] 10^5$ Wt./Vol.	Porosity (%) GRAPE	Porosity (%) Wt. H_2O / Volume	H_2O (%) Water (wt. %)	CO_3 (%) Bomb	Lithology
1-2, 47-48	1.98			1.49							1.50			2.24		71.03	47.43		marly, limy, ooze
1-2, 47-48	1.98										1.33					73.87	55.66		marly, limy, ooze
1-2, 60-61	2.11	50	12																marly, limy, ooze
2-2, 144-150	65.97										1.86					47.54	25.58		marly, limy, ooze
2-3, 28-33	66.31			1.62					1.97		1.84		3.19	2.98		43.60	23.76		marly, limy, ooze
2-3, 81-86	66.84	3.04	69	1.58	1.59	-0.01				1.90	1.90		3.00	3.00		47.72	22.96		marly, limy, ooze
2-3, 81-86	66.84											1.83				51.57	28.12		marly, limy, ooze

changes in physical properties between 580 and 600 meters suggest that an increase in wet bulk density (from 1.86-2.06 g/cm^3) actually caused a decrease in sound speed and impedance. The abrupt increase in $CaCO_3$ content (20-75%) reasonably caused the density to slow the sound speed in the absence of any increase in elastic moduli.

CORRELATION OF SEISMIC PROFILES WITH DRILLING RESULTS

Site 400 was situated on the lower rise between the Meriadzek Terrace and the Trevelyan escarpment in 4399 meters water depth (Figure 5a). Detailed multichannel seismic surveys carried out by IFP-CNEXO-CEPM (Figure 5b) show that these escarpments correspond to fault zones and that a number of buried, tilted, and rotated fault blocks existed below the rise. These blocks trend west-northwest-east-southeast and are cut by transverse faults (Montadert et. al., this volume). Well-defined parallel reflectors within the tilted blocks correspond to pre-rift sediments of Mesozoic age. The half-grabens delineated by the tilted blocks are infilled by sediments which clearly have been deposited while the blocks were rotating and are thus interpreted as syn-rift sediments. The paleotopography resulting from the rifting process was then more or less buried by unconformable sedimentary layers including a number of acoustic reflectors.

Hole 400A was drilled near the shot point 300 on the IFP-CNEXO multichannel seismic profile OC 412, near the crossing with profile OC 414 (Figure 4). These profiles were acquired using a 48-trace streamer with trace intervals of 50 meters. An implosion sound source, the Flexichoc, was used with a shot interval of 50 meters. Profile OC 412 was processed by IFP to obtain a CDP 24 stacked section and migrated.

Due to the loss of the drill string, velocity and density logs could not be run and synthetic seismograms could not be prepared. To improve the correlation between the hole and the seismics profiles, a post-leg high-resolution seismic survey was carried out by IFP-CEPM. A 24-trace streamer with 50 meters between traces was used, with a shot every 25 meters, using one micro Flexichoc as a sound source. Two profiles, GM 400 and GM 400B, crossing near the site have been processed (CDP 24 and migration). The higher frequencies recorded give a better definition in the upper part of the sedimentary sequence that was drilled, and facilitate correlation (Figure 13, 14, 15) of seismic reflectors and stratigraphy.

Because a seismic reflection depends on the acoustic impedance contrast between layers of sediments, i.e., the product of the compressional sound velocity and the wet bulk density, the best way to correlate a DSDP hole with a seismic reflection profile would be to generate a synthetic seismogram from the sonic and density loggings. This seismogram could then be compared with the seismic reflection profile. Because logging was impossible at Site 400, correlation between seismic reflectors and the lithostratigraphy has been attempted by combining several approaches.

A widely used but rather subjective approach is to assign important lithological boundaries, and especially unconformities, recognized in the hole to seismic reflectors corresponding to unconformities on the profile. By linking the absolute depth of a marker and sound travel time, a depth-travel time relationship can be derived.

On all the multichannel profiles, to the closest point to the site, one can define a succession of reflectors and seismic intervals (Figures 13 and 14). The succession of reflectors and seismic intervals picked on profiles GM 400 and 400B at the nearest point to the hole and from top to bottom is given below with reference to the regional seismic formations (Montadert et al., this volume).

Reflector	Depth (s) (2 W.t.t.)	Thickness (s) (2 W.t.t.)	Seismic Intervals	Regional Seismic Formation
Sea bottom	5820			
		0160	A	IA
1	5980	0170	B	
2	6150	0150	C	IB
3	6300	0130	D	
4	6430	0110	E	II
5	6540	0100	F	III
6	6640			

Seismic interval A is characterized by several strong reflectors, where seismic interval B is almost transparent for the frequencies used. Interval C shows a succession of weak reflectors, where interval D exhibits a succession of stronger reflectors. These four upper intervals are limited by reflector 4 which is strong and well defined. It corresponds to an unconformity on the underlying interval as it can be seen particularly well on the lines parallel to the escarp-

TABLE 5
Physical Property Summary, Holes 400/400A

Sample (Interval in cm)	Depth Sub-Bottom (m)	Strength Vane Shear (g/cm^2) Original	Strength Vane Shear (g/cm^2) Re-Mold	Sound Velocity (km/s) (Hamilton Frame) ∥ to Beds	Sound Velocity (km/s) (Hamilton Frame) ⊥ to Beds	Sound Velocity (km/s) (Hamilton Frame) Anisotropy ∥-⊥	Sound Velocity (km/s) (Hamilton Frame) Anisotropy ∥-⊥ / ⊥	C°	Wet Bulk Density (g/cm^3) GRAPE 2 Minute ∥	Wet Bulk Density (g/cm^3) GRAPE 2 Minute ⊥	Wet Bulk Density (g/cm^3) Syringe (wt./vol.)	Wet Bulk Density (g/cm^3) Chunk (wt./vol.)	Sound Impedance $\left[\frac{g}{(cm^2/s)}\right] 10^5$ GRAPE Density	Sound Impedance $\left[\frac{g}{(cm^2/s)}\right] 10^5$ Wt./Vol.	Porosity (%) GRAPE	Porosity (%) Wt. H_2O / Volume	H_2O % Water (wt. %)	CO_3 % Bomb	Lithology
Hole 400																			
1-2, 83-84	2.34	31	19					15											marly, limy, ooze
1-2, 134-140	2.87			1.47							1.50			2.21		70.34	46.90		marly, limy, ooze
1-4, 72-77	5.25	40	17	1.49							1.51			2.25		71.07	47.05		marly, limy, ooze
1-6, 140-150	8.95										1.62					67.0	41.39		marly, limy, ooze
1-6, 140-150	8.95										1.57					66.19	42.28		marly, limy, ooze
Hole 400A																			
1-1, 73-76	75.25			1.58				18				1.66		2.62		60.88	36.62	43.6	marly nannofossil ooze
1-1, 79-80	75.30	304	156																marly nannofossil ooze
2-3, 100-101	88.00	328	42																marly nannofossil ooze
2-3, 100-102	88.02			1.56	1.55	+0.01	0.01	17				1.65		2.57		62.78	38.07		marly nannofossil ooze
2-4, 140-150	88.45										1.75					58.71	33.56		marly nannofossil ooze
2-5, 98-100	90.99	245	56															49.7	nannofossil ooze
2-5, 115-121	91.19			1.59	1.54	+0.05	0.03	17	1.39	1.70		1.67	2.46	2.66		61.46	36.87	64.6	nannofossil ooze
3-3, 64-65	95.65	231	213																nannofossil ooze
3-3, 70-76	95.73			1.51	1.38	+0.13	0.09	18		1.74		1.72	2.62	2.60		58.67	34.11	56.4	nannofossil ooze
4-4, 40-44	107.92			1.55	1.55	0.0	0	20				1.73		2.68		57.84	33.63	48.7	nannofossil ooze
4-4, 80-84	108.32								1.77	1.71									nannofossil ooze
5-1, 65-68	113.17	740																	marly ooze
5-1, 65-68	113.17	1121																	marly ooze
5-1, 103-167	113.35			1.56	1.59	-0.3	-	19	1.74	1.74			2.71						marly ooze
6-1, 10-16	122.13			1.58	1.58	0.0	0	19	1.85	1.74		1.81	2.84	2.86		51.16	29.34	39.4	marly ooze
6-2, 140-150	124.95										1.38					46.14	33.33		marly ooze
6-3, 40-45	125.43			1.57	1.58	-.01	-	19	2.03	1.90		1.73	3.09	2.72		57.10	32.97	52.8	marly ooze
7-1, 82-83	132.32	1002																	nannofossil ooze
7-1, 98-103	132.55			1.57	1.57	0.0	0	19	1.90			1.75	2.98	2.75		55.85	31.85	49.7	nannofossil ooze
8-2, 58-59	141.09	710																	chalky ooze
8-2, 76-80	141.78			1.54	1.54	0.0	0	19		1.74		1.73	2.68	2.66		56.84	32.80	66.3	chalky ooze
8-4, 83-86	146.35			1.60	1.49	+11	0.07	19		1.90		1.72	2.24	2.75		58.00	33.72	55.2	chalky ooze
9-2, 81-82	150.58	553	97																chalky ooze
9-2, 91-96	151.44			1.54	1.55	-0.01	-	18	1.47				2.26					59.0	chalky ooze
9-5, 107-110	159.59			1.56	1.57	-0.01	-	19	1.41				2.20					63.2	chalky ooze
10-2, 165-108	162.54			1.91				19	1.62	1.55			3.03					51.8	chalky ooze
10-3, 5-6	163.55	969	344																chalky ooze
11-2, 51-55	169.52			1.61	1.58	+.63	0.02	19	1.90				3.06					65.3	chalky ooze
12-6, 116-117	187.59										1.74					58.83	33.91		nannofossil ooze
12-6, 140-150	167.95										1.84					54.71	29.70		nannofossil ooze
13-1, 98-99	189.49										1.55					61.26	39.42		nannofossil ooze
14-2, 133-138	266.86			1.64	1.65	-.01	-	23	1.87				3.07					77.6	nannofossil chalk
15-4, 146-150	212.48			1.60				19	1.87			2.37	2.99			22.76	9.84	70.8	nannofossil chalk
17-2, 52-54	228.53			1.59				19	1.89				3.01					73.5	nannofossil chalk
17-4, 48-52	231.50			1.60				19	1.90	1.87			3.02					72.4	nannofossil chalk
18-2, 73-78	239.26			1.58	1.60	-.02	-	20	1.79	1.88			2.90					66.3	nannofossil chalk
18-4, 140-150	241.95										1.87					50.83	27.20		nannofossil chalk
18-5, 82-86	242.84			1.62	1.59	+0.03	0.02	20	1.89	1.89			3.06					66.3	nannofossil chalk
19-2, 107-114	248.04			1.59	1.59	0.0	02	21	1.89	1.88			3.00					62.2	nannofossil chalk
20-2, 86-90	257.38			1.58	1.58	0.0	0	21	1.89	1.86			2.94					72.4	nannofossil chalk
20-5, 91-95	261.93			1.63	1.62	+0.01	0.01	21		1.90			3.10					64.2	nannofossil chalk
21-4, 138-141	270.40			1.62	1.61	.01	0.01	21	1.82				2.95					60.6	nannofossil chalk
24-5, 140-150	300.45										1.66					57.34	34.53		nannofossil chalk
24-6, 116-121	301.69			1.61	1.31	+0.30	0.23	21	1.83			1.89	2.95	3.04		48.00	25.33	73.9	nannofossil chalk
26, CC	315.9			1.64	1.62	+0.02	0.01	20	2.06	1.95		1.95	3.29	3.20		47.53	24.95	77.8	nannofossil chalk
29-1, 116-122	340.53			1.72	1.7	+0.02	0.01	21	1.97	2.00		1.98	3.41	3.41		44.03	22.30	70.5	nannofossil chalk
30-1, 30-34	350.32			1.71	1.71	0.0	0	20	2.00	1.91		1.93	3.34	3.30		46.67	24.14	85.1	nannofossil chalk
31-1, 68-72	359.57			1.61	1.61	0.0	0	20	1.93				3.10						nannofossil chalk
31-1, 122-124	360.72			1.82	1.81	+0.01	0.01	20	2.03	2.00		2.00	3.91	3.64		41.70	20.85	63.2	nannofossil chalk
34-1, 0-5	388.25			1.7				24		2.15			3.66						nannofossil chalk
35-2, 140-150	400.45										1.87					51.00	27.30		nannofossil chalk
35, CC	401.50			1.78						2.14		2.06	3.81	3.67		37.94	20.26	71.5	nannofossil chalk
36-1, 62-64	407.63											2.06				39.59	19.18	60.6	nannofossil chalk
36-1, 80-84	407.82			1.87	1.76	+0.11	0.06	20	2.19	2.10			4.01						nannofossil chalk
37-1, 94-101	417.86			1.94	1.86	+0.08	0.04	21	2.09	2.09		2.06	4.05	4.00		37.74	21.18	60.1	nannofossil chalk
37-4, 27-35	421.31			1.82	1.79	+0.03	0.02	21	2.12	2.08		1.99	3.82	3.62		42.18	18.31	58.0	nannofossil chalk
38-1, 74-78	426.76			1.94	1.84	+0.10	0.05	21	2.06	2.06			4.00						nannofossil chalk
38-1, 88-90	426.89											2.01		3.90		41.27	20.55	63.8	nannofossil chalk
39-1, 22-27	435.75			1.92	1.81	+0.11	0.06	21	2.10			2.07	4.03	3.97		39.36	19.06	62.2	nannofossil chalk
40-1, 10-14	445.12			1.97	1.87	+0.10	0.05	21	1.95	2.01		1.96	3.90	3.86		41.80	21.28	51.2	nannofossil chalk
40-1, 140-150	446.45										1.64					36.87	22.43		(siliceous)
41-1, 43-61	455.02			1.84	1.78	+0.06	0.03		1.95			1.93	3.59	3.55		43.74	22.63	47.7	(siliceous)
43-5, 94-100	480.47			1.96	1.85	+0.11	0.06	21	2.08	2.02		2.02	4.02	3.96		37.73	18.67	65.0	(siliceous)
44-1, 55-62	483.58			1.98	1.93	+0.05	0.03	21	2.08	2.04		2.05	4.08	4.06		36.78	17.96	88.3	(siliceous)
45-2, 68-76	494.72			1.88	1.83	+0.05	0.03	21	2.09	2.05		2.00	3.89	3.76		40.46	20.28	80.9	(siliceous)
45-5, 2-8	498.55			1.94	1.85	+0.09	0.05	22	2.04			2.01	3.96	3.90		39.93	19.89	29.0	(siliceous)
46-4, 101-107	507.53			1.78	1.77	+0.01	0.01	22		2.02		1.99	3.60	3.54		40.55	20.34	73.5	(siliceous)
47-6, 142-150	520.46				1.72			23	1.88	1.98		1.86	3.61	3.20		41.01	24.75	24.9	mudstone
47-7, 15-22	521.35			1.87	1.80	+0.07	0.04	23		1.96		1.90	3.67	3.55		43.84	23.08	17.0	mudstone
48-1, 143-145	522.43											1.93				43.26	22.44	7.3	mudstone
48-2, 144-150	523.47				1.56				1.90	2.00			3.04						mudstone
49-4, 90-98	535.94			1.93	1.85	+0.08	0.04	22	2.04	1.96		1.93	3.86	3.82		42.96	22.24	8.3	mudstone
50-4, 100-104	545.50			1.92	1.84	+0.68	0.04	21	1.98	1.97		1.97	3.79	3.78		40.88	20.76	33.0	mudstone

TABLE 5 – *Continued*

Sample (Interval in cm)	Depth Sub-Bottom (m)	Strength Vane Shear (g/cm^2) Original	Strength Vane Shear (g/cm^2) Re-Mold	Sound Velocity (km/s) (Hamilton Frame) ∥ to Beds	Sound Velocity (km/s) (Hamilton Frame) ⊥ to Beds	Anisotropy	Anisotropy ∥-⊥	C°	Wet Bulk Density (g/cm^3) GRAPE 2 Minute ∥	GRAPE 2 Minute ⊥	Syringe (wt./vol.)	Chunk (wt./vol.)	Sound Impedance $\left[\frac{g}{(cm^2/s)}\right] 10^5$ GRAPE Density	Sound Impedance $\left[\frac{g}{(cm^2/s)}\right] 10^5$ Wt. / Vol.	Porosity (%) GRAPE	Porosity (%) Wt. H_2O / Volume	H_2O (%) Water (wt. %)	CO_3 (%) Bomb	Lithology
Hole 400A																			
51-1, 08-14	549.61			1.93	1.85	+0.08	0.04	22	1.98	2.00		1.98	3.84	3.82		42.57	21.45	28.6	mudstone
51-2, 32-38	551.35			1.98	1.87	+0.11	0.06	22	2.16	2.09		2.03	4.21	4.02		39.26	19.33	33.2	mudstone
51-5, 100-108	556.54			1.96	1.68	+0.28	0.17	22		2.04		2.02	4.00	3.96		38.20	18.92	31.1	marly chalk
52-4, 90-98	564.44			1.84	1.91	+0.03	0.02	22	2.00	1.98		1.95	3.66	3.59		41.40	21.19	39.4	mudstone chalk
53-1, 14-20	568.67			1.82	1.78	+0.04	0.02	22	1.81	1.82		1.78	3.30	3.24		47.65	26.39	13.3	mudstone chalk
54-1, 106-116	579.11			1.88	1.83	+0.05	0.03	22	1.93	1.91		1.87	3.61	3.52		46.26	24.70	6.2	mudstone, chalk
54-3, 112-120	582.16			1.97	1.94	+0.03	0.02	22	2.04	2.03		2.04	4.01	4.02		38.09	18.64	40.4	mudstone, chalk
55-2, 47-61	584.59			1.94	1.92	+0.02	0.01	21	2.08	2.08		2.00	4.04	3.88		41.40	20.67	37.8	mudstone, chalk
56-2, 7-12	598.60			1.86	1.64	+0.22	0.13	22	2.12	2.14		2.06	3.96	3.83		36.89	17.89	82.1	marly chalk
57-1, 144-148	607.96			1.93	1.89	+0.04	0.02	22	1.90	2.19		2.06	3.75	3.98		40.86	19.83	34.5	marly chalk
59, CC	626.50			1.99	1.91	+0.08	0.04	21	2.13	2.12		2.02	4.23	4.02		34.88	17.22	63.6	marly chalk
60-6, 115-120	648.63			1.89	1.77	+0.12	0.07	22	1.98	2.05		2.01	3.81	3.80		41.19	20.47	100.00	marly chalk
62-2, 43-45	655.94																	60.0	mudstone, chalk
62-2, 136-138	656.37			1.98	1.91	+0.07	0.04	21				1.93		3.82		41.79	21.61	53.2	(dolomitic)
62-5, 130-135	661.33			1.91	1.83	+0.08	0.04	21				1.94		3.71		42.63	21.95		(dolomitic)
62-5, 140-150	661.45											2.00				41.61	20.83	48.5	(dolomitic)
63-2, 100-105	666.03			2.11	1.93	+0.18	0.09	21	1.82	1.61		1.78	3.61	3.76		43.21	24.23	46.2	(dolomitic)
63-4, 115-120	669.18			1.95	1.87	+0.08	0.04	21	1.91	1.94		1.84	3.75	3.59		41.87	22.79	50.5	(dolomitic)
64-2, 55-67	675.65			1.86	1.80	+0.06	0.03	21	2.02	2.01		1.94	3.75	3.61		43.60	22.42	40.8	(dolomitic)
64-5, 80-85	679.83			1.93	1.86	+0.07	0.04	21	1.96	1.96		1.90	3.78	3.67		43.54	22.91	31.6	(dolomitic)
65-1, 8-16	682.62			1.96	1.88	+0.08	0.04	21	1.94	1.96		1.89	3.82	3.70		44.99	23.82	21.5	(dolomitic)
66-2, 146-150	694.48			1.86	1.81	+0.05	0.03	21		1.94		1.88	3.61	3.50		50.50	26.92	29.5	(dolomitic)
66-4, 70-73	696.87			1.86	1.76	+0.10	0.06	21		2.05		1.88	3.81	3.50		48.83	25.96	24.7	(dolomitic)
68-2, 95-102	713.49			1.88	1.80	+0.09	0.04	24		1.96		1.88	3.68	3.53		50.56	26.94	44.2	(dolomitic)
68-2, 140-150	713.95											1.91				49.23	25.72	31.6	(dolomitic)
70-1																			
71-1																			
72-2, 62-64	751.13			1.91	1.81	+0.10	0.06	22	1.96	1.83		1.93	3.62	3.69		46.12	23.73	28.0	(dolomitic)
74-1, 10-13	768.12			4.35	3.79	+0.56	0.15	22	2.57	2.55			11.14						(dolomitic)

ment. Unit E, with strong reflectors, varies considerably in thickness laterally. The strong reflector 5 at its base is undulated with diffraction, suggesting an erosional surface affecting the interval F below which is almost transparent. The strong reflector 6 at its base corresponds to the boundary with the syn-rift sediments below, deposited in the half-graben.

All these seismic units exhibit lateral variations in thickness controlled by the topography inherited from the rifting episode. On profiles OC 412 or GM 400, one can observe that intervals E and F particularly, almost pinch out on the crest of the tilted block.

Thus, we have defined three main events (reflectors 4, 5, and 6) corresponding to unconformities visible on the seismic lines. By a simple comparison with the results of the hole, one can suggest that reflector 4 could correspond to an event related with an important paleoceanographic change marked by a sharp decrease of the carbonate content in the middle Eocene and a hiatus in the upper Eocene. Reflector 5 could correspond to the unconformity separating the carbonate-rich (30-70%) Upper Cretaceous-Paleocene/lower Eocene from the underlying Aptian/Albian black shales which have a low carbonate content (10-25%). Reflector 6 could not have been penetrated in Hole 400A.

A further step is to compare the depth of these events, or other changes observed in the physical properties measured on cores, with the double travel time versus depth mean curve established from velocities calculated on the seismic profile OC 412 (Figure 15). The agreement is generally good, if one takes into account the difference in location between the profiles and site and gives the following correlation between the different acoustic reflectors and the lithologies of Hole 400A.

Reflector 1 may correspond to a change in physical properties and sound impedance around 150 meters depth near the lower/upper Pliocene boundary. This change may be linked with compaction because, at this depth, nannofossil oozes begin to become chalks. However, the different reflectors in interval A correspond more probably to the alternating lithologies observed in the upper Pliocene and Quaternary section.

Reflector 2 appears well defined by several points on the travel time versus depth curve with a corresponding depth of about 300 meters. It may correspond to the increase of the sound impedance from 3 to 3.8 $[g/(cm^2\ s)]10^5$ observed at the top of the middle Miocene. This change could be also linked to a further step in the compaction of the carbonates. The homogeneous seismic character of interval B is in good accordance with the lithologic homogeneity of the upper Miocene/lower Pliocene at Hole 400A.

Reflector 3 is also very well defined on the travel time versus depth curve at a mean depth of 460 meters. We propose to correlate this reflector with the distinct increase of velocities and the lithological change observed near the middle Miocene/lower Miocene boundary around 420 meters. If this is true, the velocity and, hence depth, deduced from the curve would be too high. Therefore, the travel time versus depth curve must be corrected slightly.

Reflector 4 marks an unconformity that, following our interpretation, is related to a major paleoceanographic change occurring in the middle Eocene, with a sharp decrease of carbonate content. From the corrected travel time

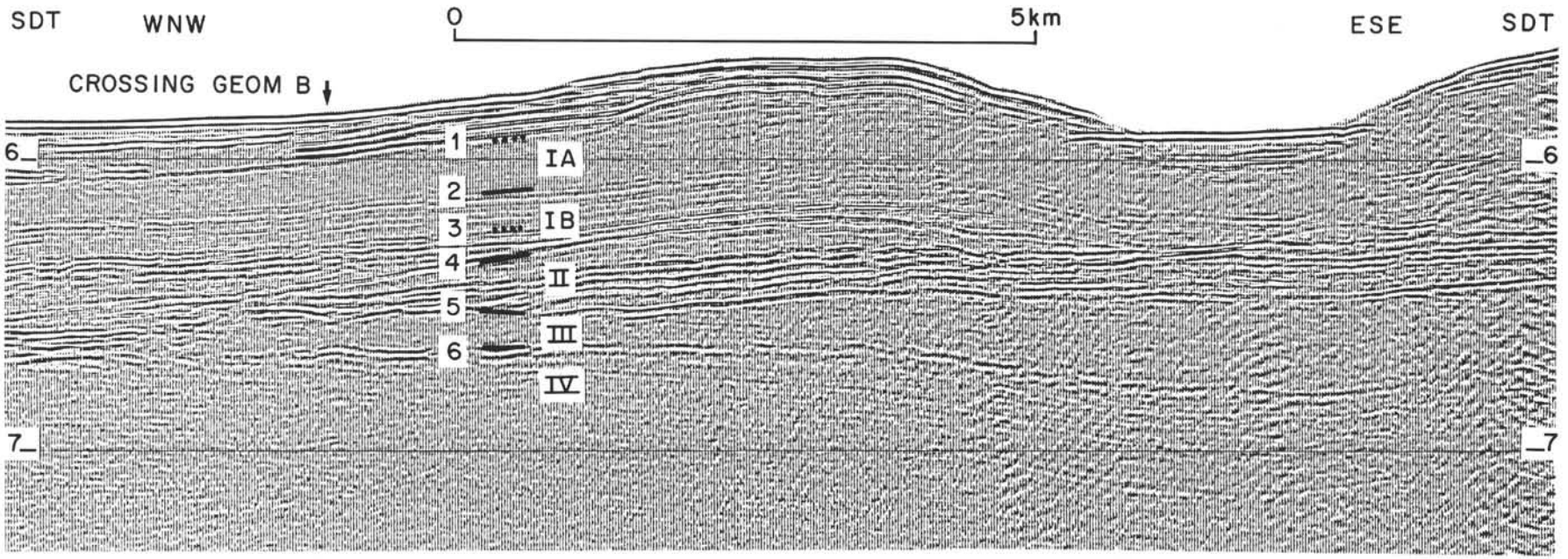

Figure 13. *Reflectors and regional seismic formations near Hole 400A on high-resolution Flexichoc multichannel seismic reflection profile GEOM 400A (IFP-CNEXO-CEPM). IA and IB = Post Eocene Cenozoic, II = Upper Cretaceous-Paleocene-Eocene, III = Aptian/Albian, IV = Pre-Aptian Lower Cretaceous.*

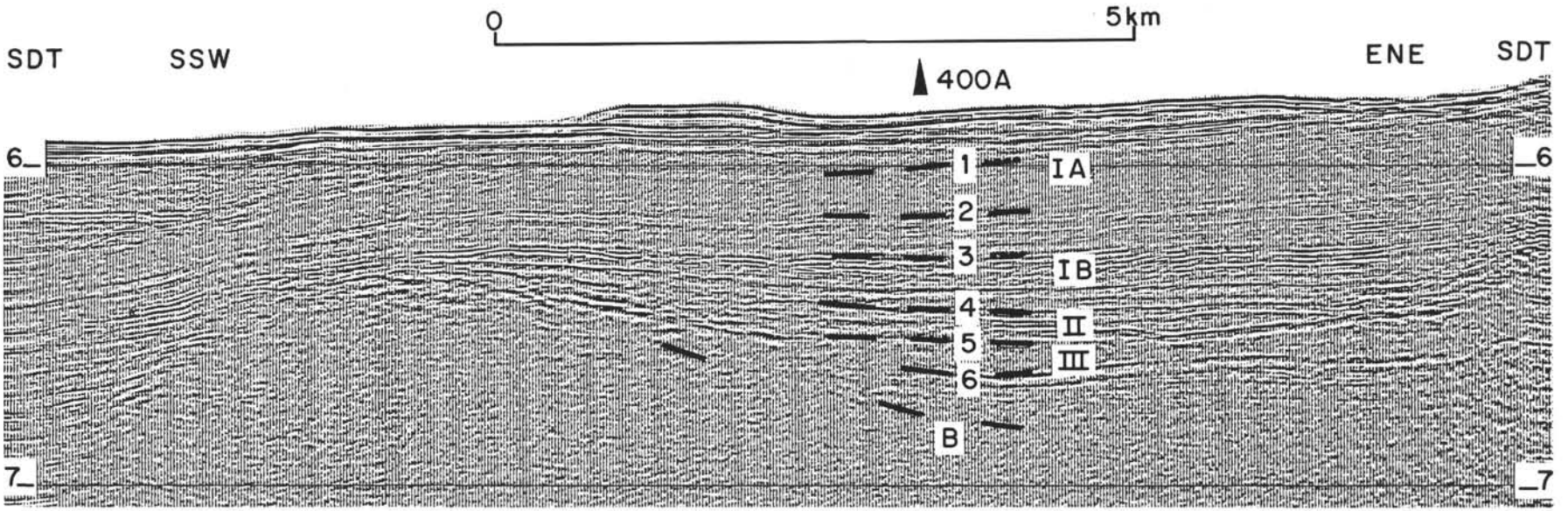

Figure 14. *Reflectors and regional seismic formations near Hole 400A on high-resolution Flexichoc multichannel seismic profile GEOM 400B (IFP-CNEXO-CEPM). IA and IB = Post Eocene Cenozoic, II = Upper Cretaceous-Paleocene-Eocene, III = Aptian/Albian, IV = Pre-rift sediments.*

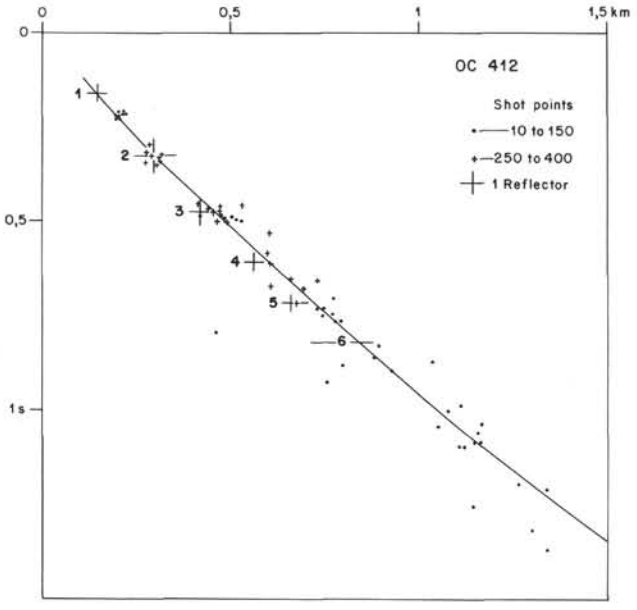

Figure 15. *Depth versus sound double travel time relationship established from velocities calculated from multichannel seismic reflection profile OC 412. Crosses 1 to 6 show location of reflectors determined from the seismic profile and the results of the hole.*

versus depth curve, it would be at around 570 meters in the middle Eocene section where important changes in acoustic impedance are observed.

Reflector 5 may correspond to an unconformity between the Upper Cretaceous and the Aptian/Albian black shales. Physical properties measured on cores confirm that at this boundary there is a drop of the acoustic impedance in relation to a decrease in carbonate content which could generate a reflection. It would be situated near 650 meters. The depth given by the travel time versus depth curve would be higher, around 730 meters and, in fact, the velocity versus depth curve does not show at this depth any decrease of veolcity as would be expected. It appears to confirm that velocities calculated from seismic reflection profiles are slightly too high and that a corrected curve must be used.

Another approach, theoretically the best, has been used, but it encounters difficulties. It consists of generating a synthetic seismogram from the velocities and densities measured on board. Velocities and densities versus depth curves are transformed into velocities and densities versus travel time curves; the impedance curve, reflection coefficient and synthetic seismogram are derived (Figure 16). The difficulties arise in establishing velocities and densities versus travel time curves. We first attempted to establish the curves assuming that one velocity measurement characterizes the velocity of the surrounding layer. However, when the sharing of the measurements is too large and the thickness of each layer is large, the velocity estimated only from one measurement must be far from its true mean velocity. The first seismogram generated did not correlate well with the seismic profile indicating that either the hole would have been much deeper than expected, or the velocities used are wrong in the upper half of the hole.

Indeed, examinations of the measurements made on board show that the values are not abundant in the upper half of the hole and sparse at the top. This distribution leads to an underestimate of the velocities and to a seismogram where reflections are too deep. To overcome this difficulty, we have introduced the constraint that reflector 5 (well defined top of the black shales on the seismic profile) must be at 0.720 s below sea bottom on the seismogram (Figure 15). The result is much more satisfactory. The synthetic seismogram is in good accord with the seismic profile, with some differences remaining for reflectors 1 and 2 (Figure 17). Therefore, in spite of the difficulties encountered, we think that this method is valuable for correlating DSDP hole results with seismic reflection profiles, provided that physical properties measurements be numerous enough especially in the unconsolidated sediments.

Table 6 summarizes the correlations proposed which are illustrated on Figure 17.

SEDIMENTATION RATES

As in the case of the other sites drilled on Leg 48, the sedimentation rate curve of Site 400 is based on age determinations derived from nannofossils and foraminifers (Figure 18). It can be observed from the figure that the sedimen-

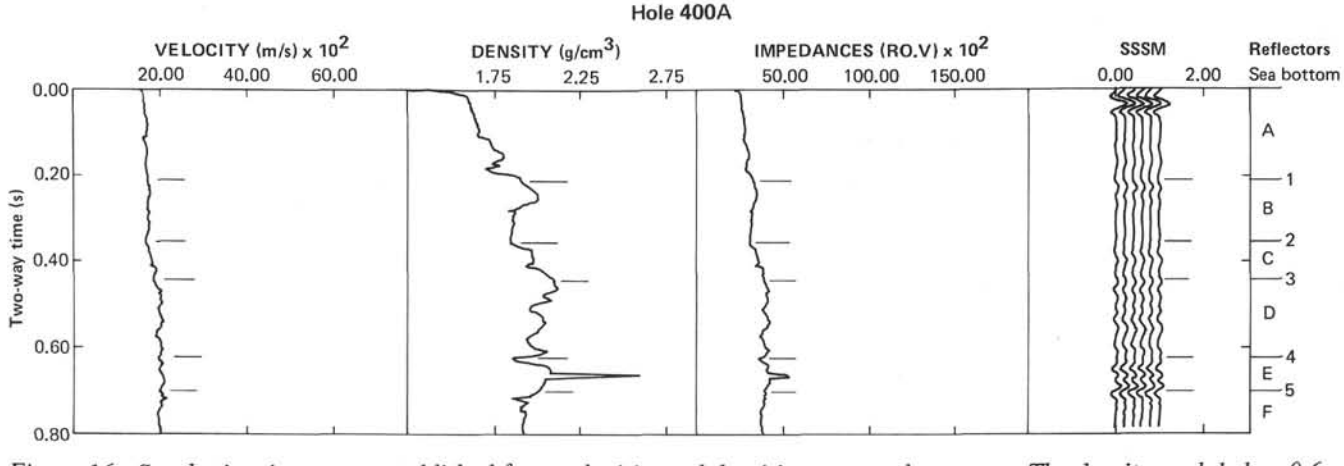

Figure 16. *Synthetic seismogram established from velocities and densities measured on cores. The density peak below 0.6 s is due to an anomalous value. Reflectors and seismic units are indicated on the right.*

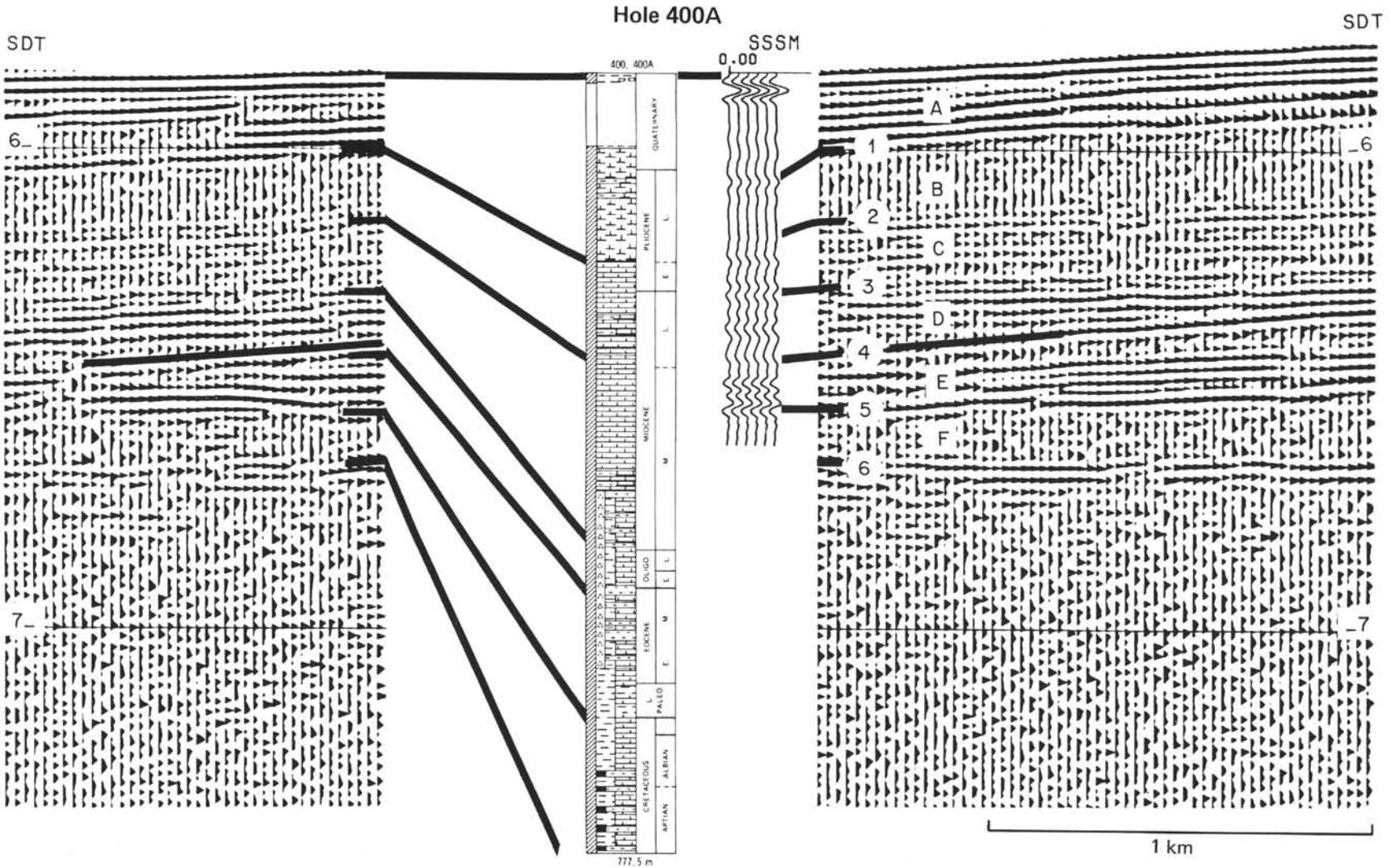

Figure 17. *Correlation of reflectors (1 to 6) and seismic units (A to F) on high-resolution seismic reflection profile GEOM 400A (IFP-CNEXO-CEPM) with synthetic seismogram and drilling results.*

TABLE 6
Correlation of Seismic Reflectors with Stratigraphic Horizons

Reflectors	2-Way Travel Time(s) Sea Level	2-Way Travel Time(s) Sea Bottom	Depth (m)	Age
Sea bottom	5820	0	0	Sea bottom
1	5980	0160	150	Early/late Pliocene
2	6150	0330	300	Top middle Miocene
3	6300	0480	420	Middle/early Miocene
4	6430	0610	570	Middle Eocene
5	6540	0720	650	Top black shales
6	6640			

tation rate for the Pliocene/Pleistocene sequence is as great as 54 m/m.y., and that a hiatus, representing an interval of about 2 m.y., may exist in the lowermost Pliocene/uppermost Miocene.

For the upper to middle Miocene, the sedimentation rate appears constant, at a rate of 22 m/m.y., which is comparatively much lower than that of the Pliocene/Pleistocene and may be due, partially, to a stronger dissolution of the calcareous microfossils. Age determinations of the lower Miocene section are not precise, making calculation of the sedimentation rate difficult. However, it is considerably lower than for the upper and middle Miocene. A small hiatus, which represents an interval of about 2 m.y., occurs within the lower Miocene.

The low sedimentation rate of 3.5 m/m.y. for the Oligocene sequence may be explained by the incomplete section. The latter is underlain by middle Eocene sediments, and the hiatus represents an interval of about 7 m.y.

Change in the sedimentation rate from 5 m/m.y. for the upper Paleocene-lowermost Eocene to 13 m/m.y. during the upper part of the lower Eocene (NP 12/NP 13) and middle Eocene is related to the lithological change from nannofossil chalk to calcareous siliceous mudstone.

A hiatus of 10 m.y. lies between the upper Paleocene and the Upper Cretaceous. Precise calculation of the sedimentation rate for the Upper Cretaceous is not possible due to the presence of cavings which represent almost the entire recovery. However, the approximate rate of 2 m/m.y. corresponds with the rate calculated for the Upper Cretaceous at Site 401. A significant hiatus, representing an interval of about 30 m.y., lies between the Upper and Lower Cretaceous.

The calculation of the sedimentation rate for the Lower Cretaceous is based on age determinations provided by foraminifers. A distinct change of the sedimentation rate can be observed at the base of the foraminifer Zone MCi 23, from about 17 m/m.y. during the Gargasian (upper Aptian) to 7 m/m.y. within the uppermost Aptian and Albian.

SUMMARY AND CONCLUSIONS

Hole 400A was drilled at the foot of the Meriadzek escarpment in the northern continental margin of the Bay of Biscay in 4399 meters of water. The continental margin is composed of several terraces and escarpments of which the most important are the Meriadzek Terrace and escarpment, and the Trevelyan escarpment situated further to the southwest near the continent-ocean boundary. Multichannel seismic profiles show a succession of tilted blocks bounded towards the southwest by rotational faults, the dips of which decrease with depth, until they become horizontal (Figure 4). A thick section of sediments is present within the tilted blocks. These sedimentary sequences include sub-parallel reflectors up to 2.0 s (4 km) in thickness that may be Permian-Jurassic pre-rift deposits, and sediments deposited during tilting of the blocks, i.e., during the rifting of the margin. Their thickness is variable and closely controlled by the blocks. Typically, they are thickest in the half-graben and thin progressively to pinch out near the crest of the block. The overlying sediments have not been affected by the faulting and are draped unconformably over the underlying rift topography.

The site was chosen from the IFP-CNEXO multichannel line OC 412 in a half-graben between two tilted blocks. The hole penetrated the post-rift section, terminating close to reflector 6 which corresponds to the unconformity that marks the end of the rifting phase. Hole 400A was continuously cored to 777.5 meters sub-bottom penetrating sediments from Holocene to late Aptian age.

Hiatuses are present probably between the lowermost Pliocene and the uppermost Miocene, within the lower Miocene, between the Oligocene and the middle Eocene, between the upper Paleocene and the Upper Cretaceous, and between the Campanian and the Albian. Four lithologic units and eight sub-units were recognized.

Description of Lithological Units

Unit 1

Unit 1 extends from the sea floor to 413 meters sub-bottom. Its base marks a small hiatus in the lower Miocene that lies close to reflector 3. Two sub-units were distinguished on the basis of changes in rates and frequency of marly beds.

Sub-Unit 1A

This sub-unit (Cores 1-6, 0-130 m) ranges in age from Quaternary to late Pliocene. It consists of a sequence of alternating nannofossil ooze and marly ooze. The carbonate content (mostly nannofossils) varies from 20 per cent to 70 per cent and decreases from bottom to top. Detrital clay-sized material comprises 25 to 50 per cent of the sediment and is dominated by illite, mixed-layer clay, with some chlorite and kaolinite. Foraminifers and siliceous microfossils comprise less than 10 per cent. Variations in color reflect small variations in the carbonate-clay ratio and degrees of oxidation. Bioturbation is intense to moderate.

Sub-Unit 1B

This sub-unit (Cores 7-36, 130-413.0 m) consists of light bluish gray to bluish white nannofossil ooze and chalk ranging in age from late Pliocene to early Miocene. They are intercalated with greenish gray marly nannofossil oozes and chalks. The carbonate content consists mainly of nannofossils, increasing from 60 per cent at the top to 8 to 85 per cent in the middle Miocene. Detrital clays and quartz average between 20 and 30 per cent. Foraminifers are common (10%) above 260 meters, but are virtually absent below. Siliceous microfossils occur sporadically. In the upper part the clays are dominated by illite and mixed-layer clays with kaolinite and chlorite; smectite increases in abundance downward with a concomitant decrease in mixed layers and chlorite, as well as quartz. There are also perturbations in the $CaCO_3$/clay ratio. In particular, a carbonate minimum

between 250 meters and 300 meters is associated with a break in biogenous silica.

In the Pleistocene, alternations of planktonic foraminiferal assemblages characteristic of the "transition zone" and subarctic zone reflect alternations in surface water masses. These cycles are less important downhole in the upper Miocene. The benthic foraminifers, which comprise as much as 30 per cent of the foraminiferal assemblages, follow these fluctuations and indicate periods of strong dissolution. The dissolution is associated with an increase in detrital sediment and biogenic silica. In the upper Miocene, the dissolution increases progressively. In mid-Miocene time the benthic fauna changed to deep-water genera and thereafter remained essentially the same until the Holocene. The Quaternary sediments are rich in nannofossils of low diversified assemblages that are typically subarctic. In the upper Pleistocene they are generally diluted by the terrigenous input associated with reworked Cretaceous and Tertiary species. However, in the lower Pleistocene and the Pliocene, they are abundant but often index species are absent or rare. In the Miocene they are abundant but poorly preserved.

Unit 2

Unit 2 (Cores 37-60, 413.0-643.0 m) ranges in age from early Miocene to late Paleocene. The base of the unit corresponds with a 7.5-m.y. hiatus between yellowish brown late Paleocene marly chalk and white marly chalk of Maestrichtian age below. Four sub-units have been differentiated on the basis of variations in biogenous silica (the concentration of which is much higher than in Unit 1), carbonate content, and sediment color. The clay mineral suite is fairly uniform and is dominated by smectite (50-60%) with illite (20-30%), kaolinite (10-15%), and chlorite (<10%).

Sub-Unit 2A

This sub-unit (Cores 37-42, 413-470 m) of early Miocene age, is dominated in the upper part by interbedded marly chalk and nannofossil chalk, with alternating light bluish gray, greenish gray, and dusky yellow-brown colors. Bioturbation is intense. Downward, siliceous remains, chiefly sponge spicules, increase in abundance with concentrations of 10 to 20 per cent and in some places as high as 40 per cent, and the lithology changes to bluish gray siliceous nannofossil chalk. Nannofossils average about 30 to 50 per cent but they are poorly preserved. Planktonic foraminifers are affected by strong dissolution which results in an enrichment of the more dissolution-resistant benthic foraminifers.

Sub-Unit 2B

This sub-unit (Cores 43-47, 470-505 m) ranges in age from early to late Oligocene. It consists of siliceous marly nannofossil chalk. The prevailing colors in the lower part are yellowish gray, yellowish brown, and grayish orange. Biogenous silica decreases while carbonate increases to around 60 per cent. The quartz content increases to 10 per cent towards the base. A high NRM intensity characterizes the base of this sub-unit. Some centimetric layers rich in foraminifers (30%) and sponge spicules (35%) exhibit horizontal lamination, cross lamination, and graded bedding. Slumping is shown by contorted laminae and exotic pebbles of contrasting lithologies of Paleocene and Early Cretaceous age. The sediments are rich in nannofossils which are badly preserved; planktonic foraminifers are strongly affected by dissolution.

Sub-Unit 2C

This sub-unit (Cores 47-55, 515-595 m) comprises siliceous mudstone of early-middle Eocene age, separated from Sub-unit 2B by a 7-m.y. hiatus. Carbonate content increases downward from 10 to 20 per cent to between 30 and 40 per cent, accompanied by a decrease in quartz content and an increase in clinoptilolite. Of significance is the presence of attapulgite and sepiolite. Color changes from yellowish gray to olive to greenish gray, light brown, and grayish orange. A corresponding sharp increase in NRM is observed. At 570 meters some laminated layers of sponge spicules are present, and slumps, microfaults, and burrows are the main sedimentary structures. Dissolution strongly affected sediments of the upper part so that they are barren of planktonic foraminifers, and even the nannofossils are strongly dissolved.

Sub-Unit 2D

This sub-unit (Cores 56-59, 595-640 m) is marked by a sharp increase in carbonate content to between 60 and 70 per cent. The section consists principally of interbedded yellowish brown marly nannofossil chalk and light greenish gray nannofossil chalk, ranging in age from late Paleocene to early Eocene. There is a marked increase in quartz and the almost complete disappearance of biogenic silica, attapulgite, and/or sepiolite. Nannofossils are abundant. Upper Paleocene sediments are rich in well-preserved planktonic and benthic foraminifers. It should be noted that the benthic foraminifer assemblages remain constant until pre-mid Miocene time and indicate deep-water conditions throughout the Cenozoic.

Unit 3

Unit 3 (Cores 60-61, 640-654 m) is separated from Unit 2 by an 8-m.y. hiatus between Maestrichtian marly nannofossil chalk and upper Paleocene marly nannofossil chalk, and from the underlying black shale of Unit 4 by a 30-m.y. hiatus between the upper Campanian and the upper Albian. It is composed of calcareous and marly nannofossil chalk with colors ranging from white to bluish white to reddish brown and grayish orange-pink. The NRM intensity remains high. In the clay fraction, smectite is abundant (50%) with zeolites (30%) and illite (10%).

The nannofossils are abundant but poorly preserved. Planktonic foraminifers are absent.

Unit 4

Unit 4 (Cores 62-74, 654-777.5 m) is characterized by alternating dark gray to black carbonaceous mudstones and greenish gray calcareous mudstones of late Albian to late Aptian age (Gargasian). Two sub-units were differentiated on the basis of abundant slumps and higher carbonate content in Sub-unit 4A and the difference in mineral as well as organic carbon content. The sub-unit boundary lies near the Albian/Aptian boundary where the sedimentation rate de-

creases from about 20 m/m.y. in Aptian time to 7 m/m.y. in Albian time.

Sub-Unit 4A

In this sub-unit (Cores 62-67, 654-711 m), Cores 64 to 67 are composed of repetitive sequences of carbonate-depleted carbonaceous claystones at the top, calcareous mudstone in the middle, and laminated silty claystones at the base. The carbonaceous claystones are mainly comprised of smectite, illite, quartz, and abundant clinoptilolite resulting from diagenetic transformation of radiolarian, diatoms, and siliceous sponge spicules. The low carbonate content (around 6%) reflects the absence of calcareous foraminifers and the presence of rare primitive arenaceous and mainly resistant species of calcareous nannoplankton. Organic carbon content is 2.4 per cent (mean value). The organic matter is of terrestrial origin (Deroo et al., this volume), and recognizable plant fragments are abundant.

In the calcareous mudstone, the carbonate content is ~23 per cent. Planktonic foraminifers are rare and few benthic calcareous foraminifers are present. Calcareous nannofossils are abundant. Clay minerals are mainly smectite and illite; diagenetic clinoptilolite is present. Organic carbon content is low (0.35%). These beds are commonly bioturbated at their top.

In the laminated silty claystones, quartz, illite, smectite, and abundant clinoptilolite have been identified. Calcareous nannofossils are abundant and planktonic foraminifers are present.

In Cores 62 to 64 the two main lithologies are light colored calcareous mudstones and silty black calcareous mudstones. These lithologies are closely interfingered by intense synsedimentary deformation with evidence of slumping. The calcareous mudstones are highly bioturbated and their carbonate content increases from 25 to 30 per cent in Core 64, Section 2 to 67 per cent in Core 62, Section 1, reflecting the presence of benthic and numerous planktonic foraminifers. Calcareous nannofossils are abundant also, but show strong signs of dissolution (Müller, this volume). The dark colored laminated mudstones which separate the slumped calcareous mudstones are composed mainly of the same components, but the grain size is somewhat coarser, and the presence of abundant plant debris is recorded by a mean organic content of about 1.8 per cent.

Sub-Unit 4B

This sub-unit (Cores 68-74, 711-777.5 m) consists of very fine grained sequences which comprise, from bottom to top, laminated silty claystones, calcareous mudstones which are bioturbated, and carbonaceous claystones. The carbonate content changes from the bottom to the top of the sequence. The laminated silty claystones and calcareous mudstones average about 30 per cent $CaCO_3$, but carbonaceous mudstones contain a maximum of only 5 per cent $CaCO_3$. In the calcareous mudstones, calcareous nannofossils and planktonic foraminifers are very abundant. In contrast, in the carbonaceous claystones, calcareous nannofossils show signs of dissolution and calcareous foraminifers are nearly absent. Radiolarian and other siliceous tests are abundant in the whole sequence, but they are practically the only biogenic remains with phosphatic (fish?) debris in the top of the sequences.

Depositional History

A series of tilted blocks bounded by rotational faults and delineating half-grabens were created during the rifting of the margin (Figure 4). Seismic reflection profiles show a thick section of pre-rift sediments of probably pre-Cretaceous age. The seismic facies of the pre-rift sequence is different from the facies observed upslope. The great number of continuous reflectors suggests alternating lithologies that may be associated with deposition in a deeper environment compared to Sites 401 and 402 where shallow water carbonates were drilled.

Sediments deposited during tilting of the blocks are presumably of Early Cretaceous age (pre-Aptian). Their thickness varies considerably from one-half graben to another. Post-rift sediments rest unconformably on a surface inherited from the rifting phase; there is no evidence of further faulting of the section. This observation has great relevance to the history of Site 400 situated at the foot of the Meriadzek escarpment. The escarpment is controlled by a large fault bounding a tilted block the crest of which was drilled at Site 401 where drill and dredge data indicate a shallow water environment during Early Cretaceous time. This implies that a considerable difference in altitude (about 1500-2000 m) already existed between Site 400 and Site 401 at the time of deposition and therefore that the post-rift black shales of Aptian-Albian age of Hole 400A were deposited in depths of at least 2000 meters. Seismic profiles show that the thickness and extent of the black shales are regionally irregular so that they are thicker in the half-grabens but are often absent on the crest of the tilted blocks.

From Hole 400A, a rhythm that can be generalized into three lithologies was observed in "the black shales" sequence. The rhythm from the bottom upwards consists of:

1) Silty claystones of dark greenish gray color that rest with sharp contact on the underlying carbonaceous mudstones but grade upwards into the calcareous mudstones. They are often finely laminated.

2) Calcareous mudstones, greenish gray to medium bluish gray in color. Burrowing is slight to moderate in the lower half and moderate to intense in the upper half.

3) Carbonaceous mudstones, medium dark gray to grayish black in color. Their lower boundary with the calcareous mudstones is generally gradational due to intense bioturbation of the upper part of the calcareous mudstone.

The average thickness of the lithologies are as follows:

	Albian	Aptian
Silty claystone	5 cm	10 cm
Calcareous mudstone	15 cm	30 cm
Carbonaceous mudstone	10 cm	10 cm
Average thickness of rhythm	30 cm	50 cm

The carbonaceous mudstones are of the same thickness throughout the Aptian/Albian sequence, whereas the two other lithologies are twice as thick in the Aptian as in the Albian. The sedimentation rate was 17 m/m.y. in the late

Aptian compared to 7 m/m.y. in the Albian (Figure 18). If allowance is made for inaccuracies in sedimentation rates due to the poor biozonation, the difference in thickness of the two lithologies observed between Aptian black shales may be ascribed to the change in sedimentation rate of calcareous mudstones. Thus, the time interval represented by each rhythm is about the same in both the Aptian and Albian and is between 20,000 to 30,000 years.

Sedimentological interpretation (de Graciansky et al., this volume) and the detailed mineralogy of other Albian sequences (Mélières, this volume) provide new insight into the origin of the black shale deposits at Site 400. The characteristics of the sequences can be explained best in terms of a model of distal turbidite deposition in deep-sea basinal conditions. The silty claystone and the overlying calcareous mudstones into which they upward grade may represent the basal part of the turbidite separated by the erosional surface of the underlying sequence. The carbonate contained in these lithologies suffered solution either at the initial site of deposition before reworking and/or during transport downslope because aragonite foraminifers are absent. However, the benthic fauna from Hole 400A is essentially the same as that found at Site 402. Because faulting of the post-Aptian sequence is not present at either site, it is concluded that the benthic fauna at Site 400 has been emplaced by downslope transport, which further supports a turbidite origin. The carbonaceous mudstones would therefore represent the terminal stage of turbidite deposition when the suspended load of fine clay and organic matter settled out slowly, allowing the carbonate to be almost completely dissolved and siliceous microfossils concentrated. The depth of burrowing also supports the emplacement of the sediment by turbidity currents since bioturbation is localized in the upper 20 to 30 cm of the calcareous mudstone and in the lower centimeters of the carbonaceous claystone. This indicates that the upper part of the sequence is to be found towards the top of the carbonaceous claystones. Because turbiditic flows are emplaced on the sea floor very quickly compared to the long span of time which separate the emplacement of two flows (around 20,000 to 30,000 years), only the upper part of the turbidite is submitted to bioturbation. The clear correlation observed between low $CaCO_3$ content and dissolution of calcareous micro- and nannofossils in the upper part of the sequence indicates that the sedimentation took place close to the CCD. This is in good agreement with the 1500 to 2000 meters water depth inferred to exist at the end of the rifting phase at Site 400. Superimposed on the short-term lithological variations related to turbidite deposition there are also clear differences related to the age of the sediments. During late Aptian time, the calcareous sediments were much more abundant than black shales. The sedimentation rate was high, and the organic carbon content low. In the early and middle Albian, the calcareous mudstones were less abundant and their $CaCO_3$ content lower due to fewer planktonic foraminifers. The sedimentation rate was low; the terrestrial influence, and thus the organic carbon content, was higher. In the late Albian, the balance was reversed again in favor of carbonate-rich chalks with a low terrestrial input. The same variations are observed at Site 402 where the Aptian/Albian black shales were deposited on a shelf. The early and middle Albian was the period of the most significant terrestrial input. Although deposited in a different deep environment, the Aptian/Albian sediments of Hole 400A reflect events recorded on the shelf. These variations were probably linked to climatic and/or tectonic events on the continent and probably affected large areas; indeed, a similar cyclic evolution has been noticed at Site 398 on the continental margin of Galicia.

We speculate that the slumping affecting the Albian sediments may be related to the oceanward tilt of the margin initiated after the onset of spreading in Biscay. Alternatively, it may also reflect a change in the physical properties of the sediments which became rich in carbonate in the late Albian. Allied to bottom currents it may be responsible for denuding the adjacent fault block of Albian sediments.

It must be pointed out that another model for deposition of Aptian/Albian at Hole 400A has been proposed (Mélières, this volume) postulating that the rhythm observed may be linked to frequent changes in dissolution rates of pelagic carbonates.

Seismic reflection profiles (Montadert et al., this volume) show that sediments seismically equivalent to the black shales of Hole 400A rest on the oceanic crust of Biscay Bay, confirming that rifting ceased just prior to their deposition. In terms of the early paleoenvironment of the bay, the absence of marine organic matter shows that the water column was not anoxic in Aptian/Albian time, although the Biscay oceanic basin was still very narrow.

A 30-m.y. hiatus separates the Albian-Aptian black shales from the Campanian/Maestrichtian nannofossil chalks and corresponds to reflector 5. This hiatus, which is contemporaneous of the global "Cenomanian" transgression, is puzzling because it separates formations that were deposited in deep waters at 400A but in shallow and deep waters at 401 and 402, respectively. An explanation based on local geological events (for example, subsidence of the margin) seems improbable because the hiatus has been found in other older parts of the Atlantic. On some seismic profiles, the overlying horizontal Upper Cretaceous section is slightly unconformable on the black shales. The unconformity may be due to deformation by differential compaction of the black shales draped over the irregular topography. Its existence suggests that the hiatus corresponds to a period of non-deposition or very slow deposition influenced by bottom currents. It could reflect reduced sediment supply due to the large Cenomanian transgression invading the flat-lying continents, which cut off any source of terrestrial material, and also to a high CCD at that time. During the missing interval, thick chalks were deposited in the epicontinental seas of northwest Europe. However, in the deeper part of the North Sea, the Cenomanian to Santonian chalks are reduced in thickness and associated with reddish brown clays. Finally, high carbonate productivity may have been essentially restricted to the very large shelf areas newly created by the Cenomanian transgression.

The Campanian/Maestrichtian above was deposited at a low sedimentation rate of about 2 m/m.y. Strong dissolution is indicated by the absence of planktonic foraminifers and the poor preservation of the nannofossils. Surface waters

were relatively cold (Létolle, this volume) and well oxygenated as indicated by the reddish and orange-pink color of the sediments.

After a 10-m.y. hiatus between Late Cretaceous and Paleocene time, lowermost Eocene chalks were slowly deposited at 5 m/m.y., but abundant and well-preserved calcareous microfossils indicate a lowering of the CCD at that time. An increase of the surface temperature is also observed (Létolle, this volume). The color of the sediments is still yellowish brown.

The overlying lower middle Eocene sediments exhibit a dramatic change marked by a strong decrease of carbonate content from 40 per cent at the base to 20 per cent at the top, with appearance of abundant biogenous silica consisting mainly of sponge spicules and radiolarians.

There is also a concomitant change from the bottom to the top from brownish colored marly chalks to greenish gray siliceous mudstones. The change is close to the lower/middle Eocene boundary and is accompanied by a sharp decrease in NRM intensity which had remained high since the Late Cretaceous. This important sedimentological change is related to a sharp rise of the CCD, indicated by the strong dissolution which affected the calcareous microfossils and caused the complete disappearance of the planktonic foraminifers. Nevertheless, there is also an increase of the sedimentation rate to 13 m/m.y. indicating an important increase in surface water productivity. This may correspond to an important change in water conditions which probably can be related to the development of deep-water circulation in the North Atlantic basin. The change is also marked by an important decrease in temperature (Grazzini et al., this volume) which affected the whole water column through the middle Eocene. The development of this circulation may explain the increased productivity and also be responsible for some erosion of the sea bottom shown by the slight unconformity with the overlying sediments. It may also be the cause of the 7-m.y hiatus separating the middle Eocene from the lower Oligocene at the site. Reflector 4 would correspond to this event. This water cooling during middle/late Eocene time seems to have a worldwide significance and generally has been related to formation of Antarctic bottom waters derived from the formation of the Antarctic ice cap and sea ice. In the case of the Bay of Biscay, the observed progressive cooling would reflect the general cooling of the oceanic waters at that time. Increasing circulation may be due also to the extension northward of the rift system which would have increased latitudinal differentiation.

After the upper Eocene hiatus, a fairly pronounced change in sedimentation occurred. The sequence of changes from the lower Oligocene to the lower Miocene is similar to that observed in the Paleocene/middle Eocene section. In the lower, and in part of the middle Oligocene, carbonates (mainly marly chalks) again become dominant, with orange to brownish colors. High NRM intensity is associated with this facies. Dissolution was still important, but some species of nannofossils indicate an influx of warmer surface waters during middle Oligocene time. Above, the color changes to greenish gray, NRM intensity becomes weak, carbonate content decreases, spicule-rich layers reappear, with evidence of bottom current activity. The early middle Oligocene could thus correspond to a slight lowering of the CCD, followed by a new rise causing strong dissolution of calcareous microfossils. Nevertheless, as was observed previously for the middle Eocene, the sedimentation rate increased from early Oligocene to early Miocene time, which may be due to higher productivity of the surface waters. This change of circulation near the middle/upper Oligocene boundary is characterized by the establishment of the psychrosphere as indicated by ostracodes (Ducasse et al., this volume).

The changes in the magnetic intensities since the Late Cretaceous are significant. High intensities were measured in Upper Cretaceous to lower Eocene and, again, in the lower Oligocene sections. They are generally associated with reddish colors of the sediments. Abrupt decreases occur near the lower middle Eocene boundary and above the lower Oligocene. This seems to correspond to important changes in water circulation. Since the dominant magnetic mineral is magnetite, most probably of detrital origin (Hailwood, this volume), these sharp decreases appear to represent an abrupt reduction in the rate of supply of magnetic minerals. It must be pointed out, however, that the upper magnetic event seems to begin slightly below the upper Eocene hiatus, presumably in the middle Eocene. This suggests that periods of deposition of highly magnetized sediments correspond essentially to periods of subaerial volcanism or to erosion of volcanics. In either case, the NRM intensity measurements appear to be an interesting tool for stratigraphic correlation. Trace elements (manganese) measurements made on carbonates (Renard et al., this volume) also suggest influence of some volcanic activity during the same period, but including the middle Eocene, in opposition to results of NRM intensity.

A 2-m.y. hiatus separates the lower Miocene from the middle Miocene deposits. During middle and late Miocene time, sedimentation was dominated by nannofossil ooze. Dissolution, with fluctuations, was still important. Nannofossils indicate warmer surface waters during the middle Miocene, followed by a strong cooling during the late part of the middle Miocene, and less important during the late Miocene. Benthic foraminiferal assemblages exhibit a complete change at this time, indicating a change in the bottom waters. This may be related to the accumulation of major ice sheets in the Antarctic.

During late Miocene/early Pliocene time, an important change occurred in which there was a trend of decreasing carbonate content due to dilution by an increasing input of terrigeneous materials, namely quartz, illite, smectite, and chlorite. The sedimentation rate became as high as 54 m/m.y. After a short warming of the surface waters at the Miocene/Pliocene boundary, temperatures progressively decreased during the Pliocene (Grazzini et al., this volume). This input of terrigeneous materials and changes in its nature testify to the deterioration of climatic conditions.

In the late Pliocene, a further cooling is represented by the almost complete extinction of discoasters and the occurrence of ice-rafted materials. During the Pleistocene, large variations of water temperatures are recorded (Grazzini et al., this volume) associated with variations of

foraminiferal and nannofossils assemblages. Associated facies changes reflect fluctuations in the clay/carbonate ratio.

The seismic, sedimentological, and biostratigraphic data show that the depth of deposition at Site 400 was about 2000 meters in Aptian/Albian time at the onset of spreading and the end of rifting. Depths comparable to the present have been in existence since the beginning of the Cenozoic due to the thermal subsidence of the margin.

REFERENCES

Bacon, M. and Gray, F., 1971. Evidence for crust in the deep ocean derived from continental crust, *Nature*, v. 229, no. 5283, p. 331-332.

Bacon, M., Gray, F., and Matthews, D.H., 1969. Crustal structure studies in the Bay of Biscay, *Earth Planet. Sci. Lett.*, v. 6, no. 5, p. 377-385.

Bé, A.W.H. and Tolderlund, D.S., 1971. Distribution and ecology of living planktonic foraminifera in surface waters of the Atlantic and Indian oceans. *In* Funnell, B.M. and Riedel, W.R. (Eds.), *Micropaleontology of oceans:* Cambridge (Cambridge Univ. Press), p. 105-149.

Berthois, L. and Brenot, R., 1964. Bathymétrie du golfe de Gascogne et de la côte du Portugal. I. Commentaires sur le levé complémentaire des feuilles no. 9 et 10 des abords du plateau continental. II. Bathymétrie du talus du plateau continental à l'ouest de la péninsule ibérique du cap Finisterre au cap Saint Vincent, *Cons. Int. Explor. Mer,* P.-V. de la 52nd réunion, Sept.-Oct., 1964.

Berthois, L., Brenot, R., and Ailloud, P., 1965. Essai d'interprétation morphologique et tectonique des levés bathymétriques exécutés dans la partie sud-est du golfe de Gascogne, *Rev. Trav. Inst. Pêches marit.*, v. 29, p. 343-345.

Boillot, G. and Capdevila, R., 1977. The Pyrénées: subduction and collision ?, *Earth Planet. Sci. Lett.*, v. 35, no. 1, p. 151-160.

Boillot, G., Dupeuble, P.A., Lamboy, M., d'Ozouville, L., and Sibuet, J.C., 1971. Structure géologique de la marge continentale asturienne et cantabrique (Espagne du Nord). *In Histoire structurale du golfe de Gascogne:* Paris (Ed. Technip), V. I-II, p. V, 6-1-V6-52.

Bullard, E.C., Everett, J.E., and Smith, A.G., 1965. The fit of the continents around the Atlantic, *Phil. Trans. Roy. Soc. London,* ser. A, v. 258, p. 41-51.

Carey, S.W., 1955. A tectonic approach to continental drift, *Symp. Cont. Drift,* Univ. Tasmania, p. 177-355.

Cholet, J., Damotte, B., Grau, G., Debyser, J., and Montadert, L., 1968. Recherches préliminaires sur la structure géologique de la marge continentale du golfe de Gascogne. Commentaires sur quelques profils de sismique réflexion "Flexotir," *Rev. Inst. Franc. Pétrole,* v. 23, p. 1029-1045.

Choukroune, P., Le Pichon, X., Seguret, M., and Sibuet, J.C., 1973. Bay of Biscay and Pyrenees, *Earth Planet. Sci. Lett.*, v. 18, p. 109-118.

Curry, D., Hamilton, D., and Smith, A.J., 1971. Geological evolution of the western English Channel and its relation to the nearby continental margin, *Nat. Env. Res. Council, Inst. Geol. Sci., Rept. 70/14 (ICSU/SCOR working party 31 Symp.),* Cambridge 1970, p. 129-142.

Damotte, B., Debyser, J., Montadert, L., and Delteil, J.R., 1969. Nouvelles données structurales sur le golfe de Gascogne obtenues par sismique réflexion "Flexotir." Communication présentée au Colloque du CNRS, Villefranche-sur-mer, Mocano, Sept. 1968, *Rev. Inst. Franc. Pétrole,* v. 9, p. 1029-1060.

Dardel, R.A. and Rosset, R., 1971. Histoire géologique et structurale du bassin de Parentis et de son prolongement en mer. *In Histoire structurale du Golfe de Gascogne:* Paris (Ed. Technip), v. 1, p. IV. 2-1-IV. 2-28.

Girdler, R.W., 1965. Continental drift and the rotation of Spain, *Nature,* v. 207, no. 4995, p. 396-398.

Grau, G., Montadert, L., Delteil, R., and Winnock, E., 1973. Structure of the European continental margin between Portugal and Ireland, from seismic data. *In* Mueller, S. (Ed.), *The structure of the earth's crust: Tectonophysics,* v. 20, p. 319-339.

Harker, S.D. and Sarjeant, W.A.S., 1975. The stratigraphic distribution of organic-walled dinoflagellate cysts in the Cretaceous and Tertiary, *Rev. Palaeobot. Palynol,* v. 20, p. 217-315.

Hersey, J.B. and Whittard, W.F., 1966. The geology of the Western Approaches of the English Channel: V. The continental margin and shelf under the south Celtic Sea. *In Continental margins and island arcs: Geol. Survey Canada Paper 66-15,* p. 80-106.

Hill, M.N. and Vine, F.J., 1965. A preliminary magnetic survey of the Western Approaches to the English Channel, *Quart. J. Geol. Soc. London,* v. 121, p. 463-475.

Lapierre, F., 1972. Etude structurale du plateau continental à l'Ouest de la Bretagne, *Rev. Inst. Franc. Pétrole Ann. Combust. Liquides,* v. 27, p. 73-89.

Laughton, A.S., Berggren, W.A., et al., 1972. *Initial Reports of the Deep Sea Drilling Project,* v. 12: Washington (U.S. Government Printing Office).

Laughton, A.S., Roberts, D.G., and Graves, R., 1975. Bathymetry of the northeast Atlantic: Mid-Atlantic Ridge to southwest Europe, *Deep-sea Res.*, v. 22, p. 791-810.

Le Mouel, J.L. and Le Borgne, E., 1971. La cartographie magnétique du golfe de Gascogne. *In Histoire structurale du golfe de Gascogne:* Paris (Ed. Technip), v. I-II, p. VI. 3-1-VI. 3-12.

Le Pichon, X., Bonnin, J., Francheteau, J., and Sibuet, J.C., 1971. Une Hypothèse d'évolution tectonique du golfe du Gascogne. *In Histoire structurale du golfe de Gascogne:* Paris (Ed. Technip), v. I-II, p. VI.11-1-VI.11-44.

Limond, W.Q., Gray, F., Grau, G., and Patriat, P., 1972. Mantle reflections in the Bay of Biscay, *Earth Planet. Sci. Lett.*, v. 15, no. 4, p. 361-366.

Matthews, D.H. and Williams, C.A., 1968. Linear magnetic anomalies in the Bay of Biscay: a qualitative interpretation, *Earth Planet. Sci. Lett.*, v. 4, no. 4, p. 315-320.

Montadert, L. and Winnock, E., 1971. L'histoire structurale du golfe de Gascogne. *In Histoire structurale du golfe de Gascogne:* Paris (Ed. Technip), v. I-II, p. VI.16-1-VI.16-18.

Montadert, L., Damotte, B., Debyser, J., Fail, J.P., Delteil, J.R., and Valéry, P., 1971a. Continental margin in the Bay of Biscay. *In* Delany, F.M. (Ed.), *The geology of the East Atlantic continental margin: Inst. Geol. Sci. Rept. 70/15,* p. 43-74.

Montadert, L., Damotte, B., Delteil, J.R., Valéry, P., and Winnock, E., 1971b. Structure géologique de la marge continentale septentrionale du golfe de Gascogne (Bretagne et Entrées de la Mancye). *In Histoire structurale du golfe de Gascogne:* Paris (Ed. Technip), v. I-II, p. III.2-1-III.2-22.

Montadert, L., Damotte, B., Fail, J.P., Delteil, J.R., and Válery, P., 1971c. Structure géologique de la marge continentale asturienne et cantabrique (Espagne du Nord). *In Histoire structurale du golfe de Gascogne:* Paris (Ed. Technip), v. I-II, p. V.7-1-V.7-16.

Montadert, L., Damotte, B., Fail, J.P., Delteil, J.R., and Valéry, P., 1971d. Structure géologique de la plaine abyssale du golfe de Gascogne. *In Histoire structurale du golfe de Gascogne:* Paris (Ed. Technip), v. I-II, p. VI.14-1-VI.14-42.

Montadert, L., Winnock, E., Delteil, J.R., and Grau, G., 1974. Continental margins of Galicia-Portugal and Bay of Biscay. *In* Burk, C.A. and Drake, C.L. (Eds.), *The geology of continental margins:* New York (Springer-Verlag), p. 323-342.

Pastouret, L. and Auffret, G.A., 1975. Observations sur les microfaciès des roches sédimentaires prélevées sur la marge amoricaine, *Rev. I.F.P.*, v. 31, p. 401-425.

Pastouret, L., Masse, J.-P., Philip, J., and Auffret, G.A., 1974. Sur la présence d'Aptien inférieur à faciès urgonien sur la marge continentale armoricaine. Conséquences paléogéographiques, *C. R. Acad. Sci. Paris,* ser. D, v. 278, p. 2011-2014.

Pautot, G., Renard, V., de Charpal, O., Auffret, G.A., and Pastouret, L., 1976. A granite cliff deep on the North Atlantic, *Nature,* v. 263, p. 669-672.

Reid, P.C. and Harland, R., in press. North Atlantic, Quaternary dinoflagellate cyst studies, *Am. Assoc. Stratig. Palynol. Contrib.*

Schnitker, D., 1974. West Atlantic abyssal circulation during the past 120,000 years, *Nature,* v. 248, p. 385-387.

Sibuet, J.C. and Le Pichon, X., 1971. Structure gravimétrique du golfe de Gascogne et le fossé marginal nord-espagnol. *In Histoire structurale du golfe de Gascogne:* Paris (Ed. Technip), v. I-II, p. VI.0-1-VI.9-18.

Sibuet, J.C., Pautot, G., and Le Pichon, X., 1971. Interprétation structurale du golfe de Gascogne à partir des profils de sismique. *In Histoire structurale du golfe de Gascogne:* Paris (Ed. Technip), v. I-II, p. VI.10-1-VI.10-32.

Smith, S.G. and Van Reissen, E.D., 1973. The Meriadzek terrace: a marginal plateau, *Marine Geophys. Res.*, v. 2, p. 83-94.

Stauffer, K.W. and Tarling, D.H., 1971. Age of the Bay of Biscay: New paleomagnetic evidence. *In Histoire structurale du Golfe de Gascogne:* Paris (Ed. Technip), v. 1, p. II.2-1-II.2-18.

Storetvedt, K.M., 1970. Paleomagnetism of the Lisbon volcanics. A discussion of a recent paper by N.D. Watkins and A. Richardson, *Geophys. J. Roy. Astron. Soc.*, v. 19, p. 107-110.

Streeter, S.S., 1973. Bottom water and benthonic foraminifera in the North Atlantic-Glacial-Interglacial contrasts, *Quat. Res.*, v. 2, p. 38-69.

Stride, A.H., Curray, J.R., Moore, D.G., and Belderson, R.H., 1969. Marine geology of the Atlantic continental margin of Europe, *Phil. Trans. Roy. Soc. London,* ser. A, v. 264, p. 31-75.

Van der Voo, R., 1968. Comments on paleomagnetism of the Lisbon volcanics by N.D. Watkins and A. Richardson, *Geophys. J. Roy. Astron. Soc.*, v. 16, p. 543-547.

Van der Voo, R. and Zijderveld, J.D.A., 1971. Renewed paleomagnetic study of the Lisbon volcanics and implications for the rotation of the Iberian Peninsula, *J. Geophys. Res.*, v. 76, p. 3913-3921.

Watkins, N.D. and Richardson, A., 1968. Paleomagnetism of the Lisbon volcanics, *Geophys. J. Roy. Astron. Soc.*, v. 15, p. 287-304.

Winnock, E., 1971. Géologie succincte de bassin d'Aquitaine (contribution à l'histoire du golfe de Gascogne). *In Histoire structurale du golfe de Gascogne:* Paris (Ed. Technip), v. I-II, p. IV.1-1-IV.1-30.